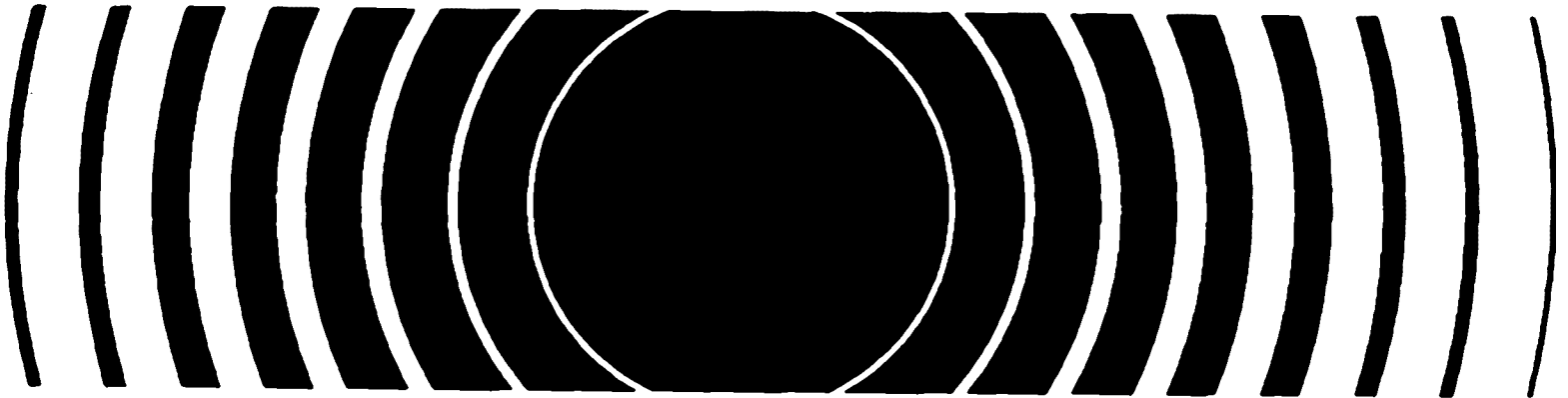**&EPA**

Analysis And Evaluation Of A Radioactive Waste Package Retrieved From The Atlantic 3800-Meter Low-Level Radioactive Waste Disposal Site

ANALYSIS AND EVALUATION OF A RADIOACTIVE WASTE PACKAGE RETRIEVED FROM THE ATLANTIC 3800-METER LOW-LEVEL RADIOACTIVE WASTE DISPOSAL SITE

Prepared for the U.S. Environmental Protection Agency

by

P. Colombo, M.W. Kendig, M. Fuhrmann
Environmental and Waste Technology Center
Department of Nuclear Energy, Brookhaven National Laboratory
Upton, New York 11973

August 1993

FOREWORD

From 1946 to 1970 the United States used designated ocean sites for disposal of radioactive wastes. In 1974 the Environmental Protection Agency's (EPA) Office of Radiation and Indoor Air (ORIA) initiated a program to determine the potential for any adverse human health or environmental impacts resulting from previous ocean disposal of radioactive waste materials, or from radiation contamination due to other events such as the Chernobyl nuclear power plant accident. This program of wide-ranging monitoring and assessment studies characterized natural environmental parameters in and near disposal sites or depositional areas and identified and evaluated concentrations and distributions of radionuclides.

Additionally, beginning in 1976, the ORIA initiated studies to determine whether existing technologies could be applied toward assessing the fate of radioactive waste packages that had been previously deposited on the seafloor in disposal sites. After successfully locating clusters of radioactive waste packages in three deep-ocean disposal sites, one package was retrieved from each site to evaluate the performance, with time, of past packaging techniques. Under an interagency agreement with ORIA, the Brookhaven National Laboratory (BNL) has performed container corrosion and matrix analysis studies on the three recovered packages. The results of previous BNL analyses of two waste packages were published in EPA Technical Reports "Analysis and Evaluation of a Recovered Radioactive Waste Package from the Atlantic 2800-Meter Disposal Site" (EPA 520/1-82-009), and "Analysis and Evaluation of a Recovered Radioactive Waste Package Retrieved from the Farallon Islands 900-Meter Disposal Site" (EPA 520/1-90-014). This report details the results of the analysis of a radioactive waste package recovered from the Atlantic Ocean 3800-meter disposal site in 1978.

These three reports and the previously published EPA Technical Report "Recovery of Low-Level Radioactive Waste Packages from Deep-Ocean Disposal Sites" (EPA 520/1-90-027) may be particularly helpful at this time because of recent information made public by Russia regarding past dumping or disposal activities by the former Soviet Union of radioactive waste and radioactive equipment/materials in the Kara and Barents Seas.

Readers of this report are invited to send comments/suggestions to Mr. Eugene Durman, Acting Director, Radiation Studies Division (6603J), Office of Radiation and Indoor Air, U.S. Environmental Protection Agency, Washington, DC, 20460.
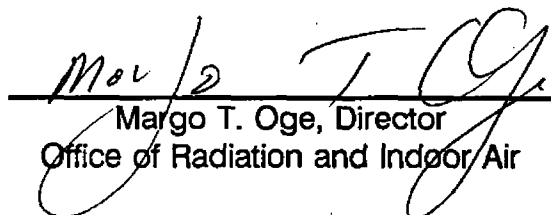
Margo T. Oge, Director
Office of Radiation and Indoor Air

iii

TABLE OF CONTENTS

LIST OF FIGURES

LIST OF FIGURES (continued)

LIST OF TABLES

1. DESCRIPTION OF ATLANTIC 3800-METER RADIOACTIVE DISPOSAL SITE

In June, 1978, the Office of Radiation Programs, U.S. Environmental Protection Agency, conducted a monitoring program at the Atlantic 3800-meter radioactive waste disposal site. A major objective of this study was to locate radioactive waste packages and to identify and recover a typical package to determine the effects of the ocean environment on the chemical and physical properties of the package over the period of time it was on the ocean bottom. Similar surveys were conducted at the Atlantic 2800-meter radioactive disposal site in 1976 [1], and at the Pacific Farallon Islands 900-meter site in 1977 [2].

The Atlantic 3800-meter site is located approximately 320 kilometers off the mainland coast on the lower continental rise, 260 kilometers seaward of the edge of the continental shelf, near the main channel of the Hudson submarine canyon system (Figure 1). This study was conducted in the area of coordinates 37°38'N and 70°35'W, covering an area on the lower continental rise near the confluence of the main channels of the Hudson and Block submarine canyon systems.

In this region, the channel of the Hudson Canyon is characterized by an approximately 1-kilometer wide canyon floor that contains a narrow, deeper, meandering thalweg or axis. The walls that bound the canyon floor vary from gentle sloping to vertical and are about 200 meters high. In this area, water depths vary from 3700 to 4100 meters [3].

The 3800-meter site was used between 1957 and 1959, during which time it received an estimated 14,500 waste packages having a total estimated activity of 2,100 curies of mixed fission products (Table 1). Most of the disposed wastes were generated by government and commercial nuclear facilities along the eastern part of the United States.
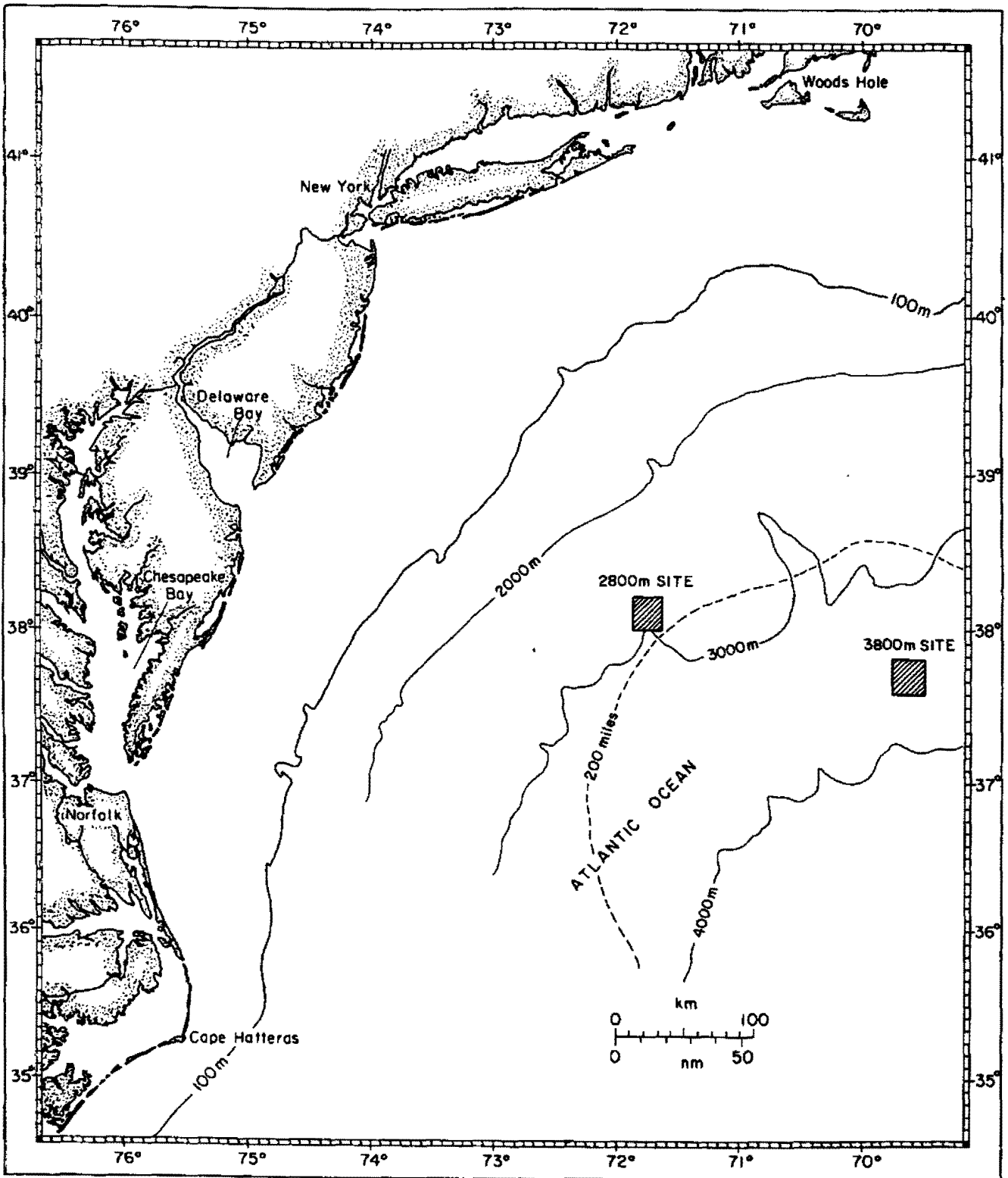
Figure 1   Major U.S. Radioactive Waste Disposal Sites in the Atlantic Ocean

Site	Coordinates (Center of Site)	Depth (m)	Distance from Land (km)	Years Disposal Site Used	Estimated No. of Disposed 55-Gallon Drums	Estimated Activity in Drums at Time of Disposal (Ci)	(T Bq)
						Table 1 Primary United States Ocean Disposal Sites for Low-Level Radioactive Waste	
Atlantic	38°30'N 72°06'W	2800	190	1951-1956 1959-1962	14,300	41,400[a]	(1530)
Atlantic	37°38'N 70°35'W	3800	320	1957-1959	14,500	2,100	(77.7)
Pacific Farallon Islands	37°38'N 123°08'W	900	60	1951-1953	3,500	1,100	(40.7)
Farallon Islands	37°37'N 123°17'W	1700	77	1946-1950 1954-1965	44,000	13,400	(496)

[a] This does not include the pressure vessel of the N/S Seawolf reactor with an estimated induced activity of 33,000 Ci. (1220 T Bq)

2. WASTE PACKAGE SURVEY AND RETRIEVAL OPERATIONS

The recovery of the waste package from the Atlantic 3800-meter disposal site was a coordinated effort involving the DSV ALVIN, its mother ship R/V LULU, and the R/V ADVANCE II which was designated for shipboard recovery of a radioactive waste package. The R/V ADVANCE II also served for collecting biological, geological and radiochemical data relevant to the characteristics of the disposal site.

On June 23 and 24, 1978, two dives were made with the DSV ALVIN (dives #812, 813), to locate a region containing radioactive waste packages. The first radioactive waste package was observed at a depth of 3970 meters (Figure 2). A prominent scour moat was present on the up-current side of the package and a mound of granule-sized sediment had built up on the down-current side of the package. The package appeared intact with signs of corrosion and blistering on the exposed bottom rim of the mild steel container (Figure 3). Currents, flowing southwesterly, were estimated at a velocity of 25 to 30 cm/sec. These strong currents have kept the upper surface of this container free of sediment accumulation. Soft marl talus littered the local area of this package. The water was turbid but slightly clearer than the water higher on the channel wall [3]. Identification marks on the container were not detectable, probably due to corrosion.

During the course of the survey, a package having distinguishable markings was located (Figure 4). The number 953 was painted, in yellow, near the upper rim of the container. The package was surrounded by a well-defined scour moat similar to that found around the package described earlier (Figure 2). The bottom side of the container had a wedge of sediment sloping away from it, which was probably formed when the package slid into its present position, plowing up the sediment as it moved. The drums located during dive #813 appear to be lying near the base of the eastern side of the Hudson submarine canyon channel, on the lower continental rise, at a depth of 3970 meters.

5
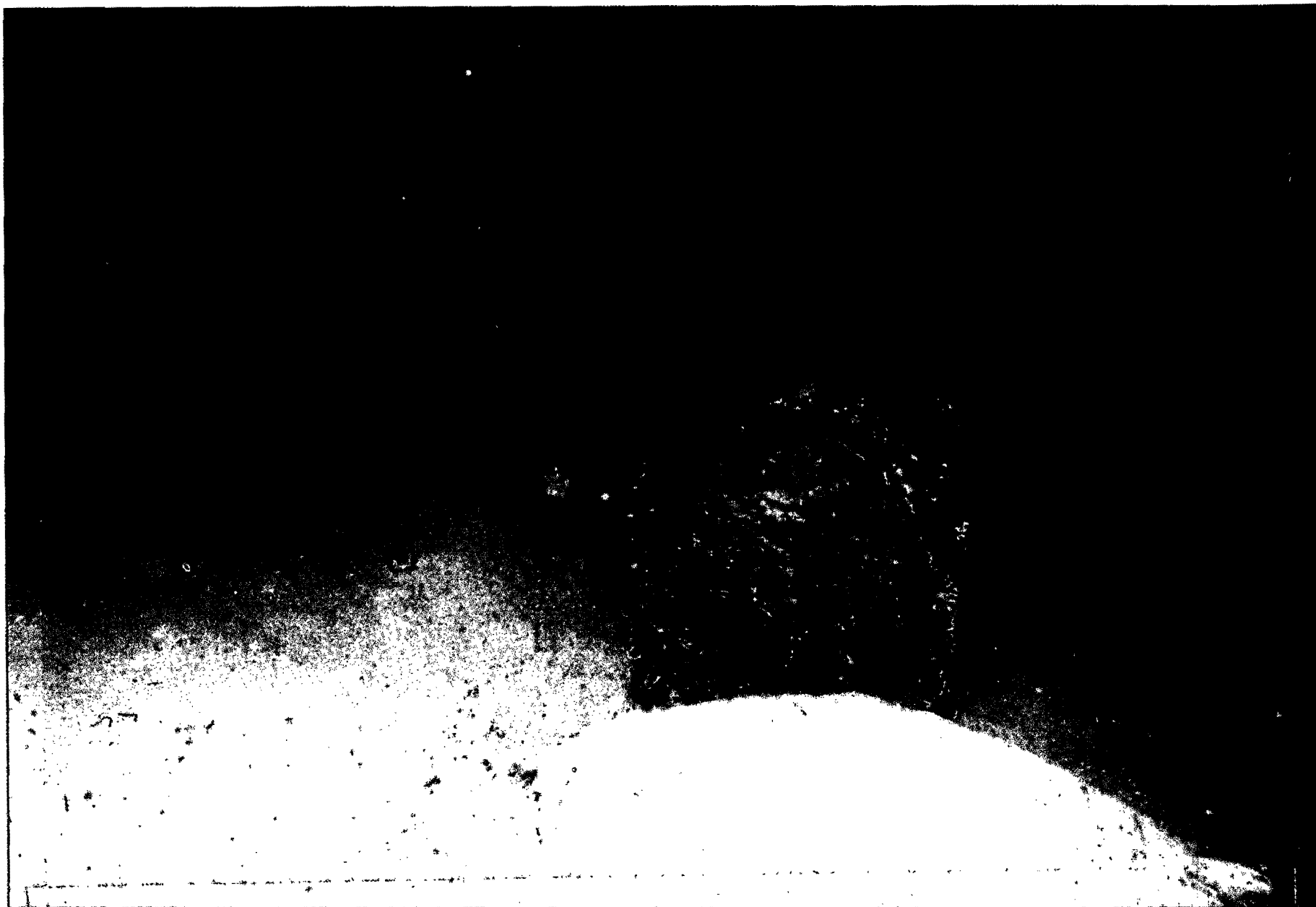
Figure 2   A radioactive waste package observed at a depth of 3,970 meters.

Figure 3   A close-up of the package in Figure 2 appears intact with signs of corrosion and blistering on the exposed bottom rim.
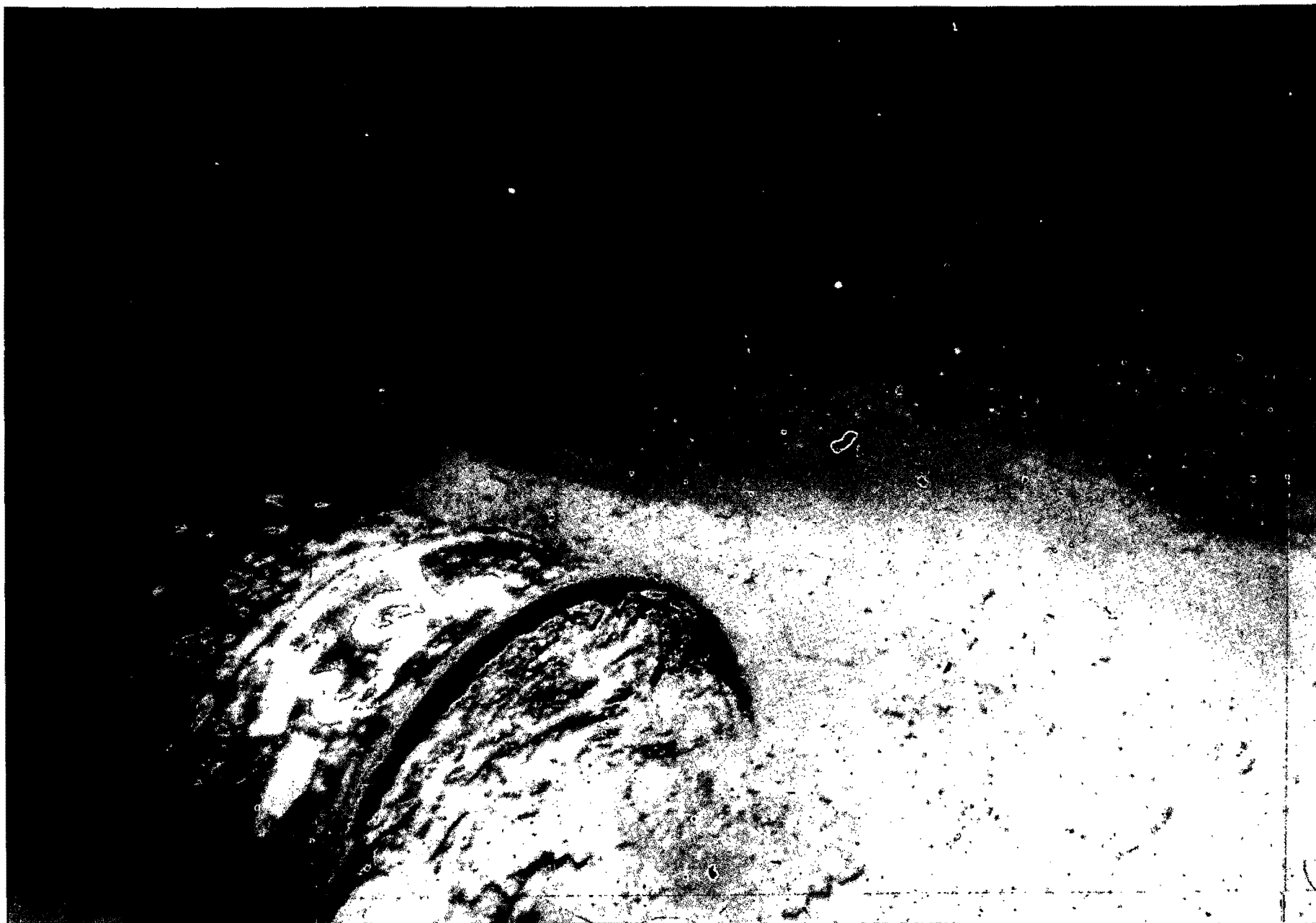
Figure 4   A waste package having a distinguishable marking was located at a depth of 3,970 meters surrounded by a scour moat.

2. WASTE PACKAGE SURVEY AND RETRIEVAL OPERATIONS

The recovery of a waste package from the Atlantic 3800-meter site involved using DSV ALVIN, its mother ship R/V LULU, and R/V ADVANCE II. The ADVANCE II would receive the recovered package from the ALVIN, and would also collect environmental data to characterize the disposal site.

On June 23 and 24, DSV ALVIN made two dives (#812, 813), to locate a region containing radioactive waste packages. The first package was observed at 3970 meters depth (Figure 2). A prominent scour moat was present on its up-current side and a mound of granule-sized sediment had built up on its down-current side. The package appeared intact with signs of corrosion and blistering on the exposed bottom rim of the mild steel container (Figure 3). Identification marks were not detectable, probably due to corrosion. Currents, flowing southwesterly, were estimated at 25 to 30 cm/sec. These strong currents kept the upper surface of this container free of sediment accumulation. Soft marl talus littered the local area of this package. The water was turbid but slightly clearer than the water higher on the channel wall [3].

Another package with distinguishable markings was also located (Figure 4). The number 953 was painted, in yellow, near its upper rim. This package was surrounded by a well-defined scour moat similar to that described earlier (Figure 2). Its bottom side had a wedge of sediment sloping away from it -- probably formed when it slid into its present position, plowing up the sediment as it moved. Drums located during dive #813 were lying near the base of the eastern side of the Hudson submarine canyon channel, on the lower continental rise, at a depth of 3970 meters.

It was decided to recover waste package "953" due to its identifiable markings and its apparent physical suitability for a successful retrieval. The position of the waste package was fixed, utilizing the ALNAV navigation system operated from the R/V LULU [4].
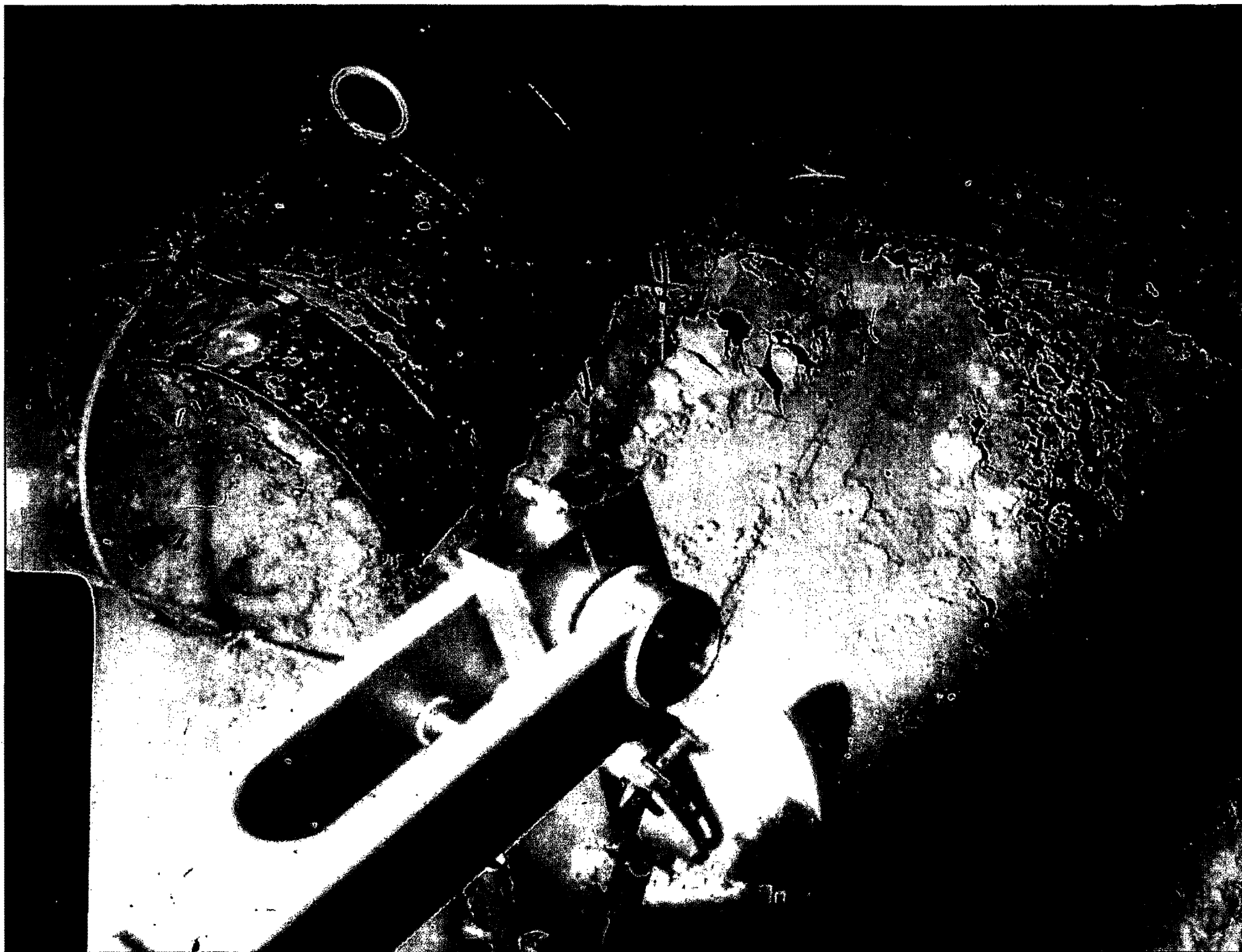
Figure 5   Retrieval operations using ALVINs mechanical arm to place a metal harness around the waste package.

2.2 Waste Package Retrieval Operations

In the morning of June 25, 1978, ALVIN was launched to recover the marked (953) package located by the submersible during dive 813. Preparations were made for a direct lift recovery, similar to that used for the waste package recovery at the Farallon Islands 900-meter disposal site in 1977 [2,4]. This included the removal of non-essential scientific equipment on the ALVIN, installation of releasable lift equipment and the addition of syntactic foam flotation material in conformance with ALVIN's lifting capacity.

Descent to the 3970-meter depth location of the selected waste package took approximately two hours. On locating the package, ALVIN proceeded to capture it by placing a metal harness around it using the ALVIN's mechanical arm (Figure 5). The same harnessing procedure was used during the recovery of a waste package from the Atlantic 2800-meter site in 1976 [1]. A 100-meter tag line was attached between the eye of the harness and an attachment point underneath the submersible using explosive bolts for emergency release purposes [4]. The ascent to the surface took three hours, with a total dive time of six and one-half hours. After ALVIN surfaced, a lift line was extended from the stern-mounted A-frame of the R/V ADVANCE II to the tag line attached to ALVIN's underside. The package was released from the ALVIN, and recovery operations aboard the ADVANCE II began. After clearing the surface, and before taking the waste package aboard, it was allowed to drain to minimize shipboard contamination (Figure 6). During that time, it was subjected to a radiation survey by health physicists aboard the ADVANCE II.

Immediately following the survey, the package was taken aboard, where it was photographed and carefully examined for biological growth and corrosion products. Within one-hour the package was transferred to a sealed storage container under a positive pressure of argon gas to inhibit or retard further corrosion prior to analysis at Brookhaven National Laboratory (Figure 7).

11
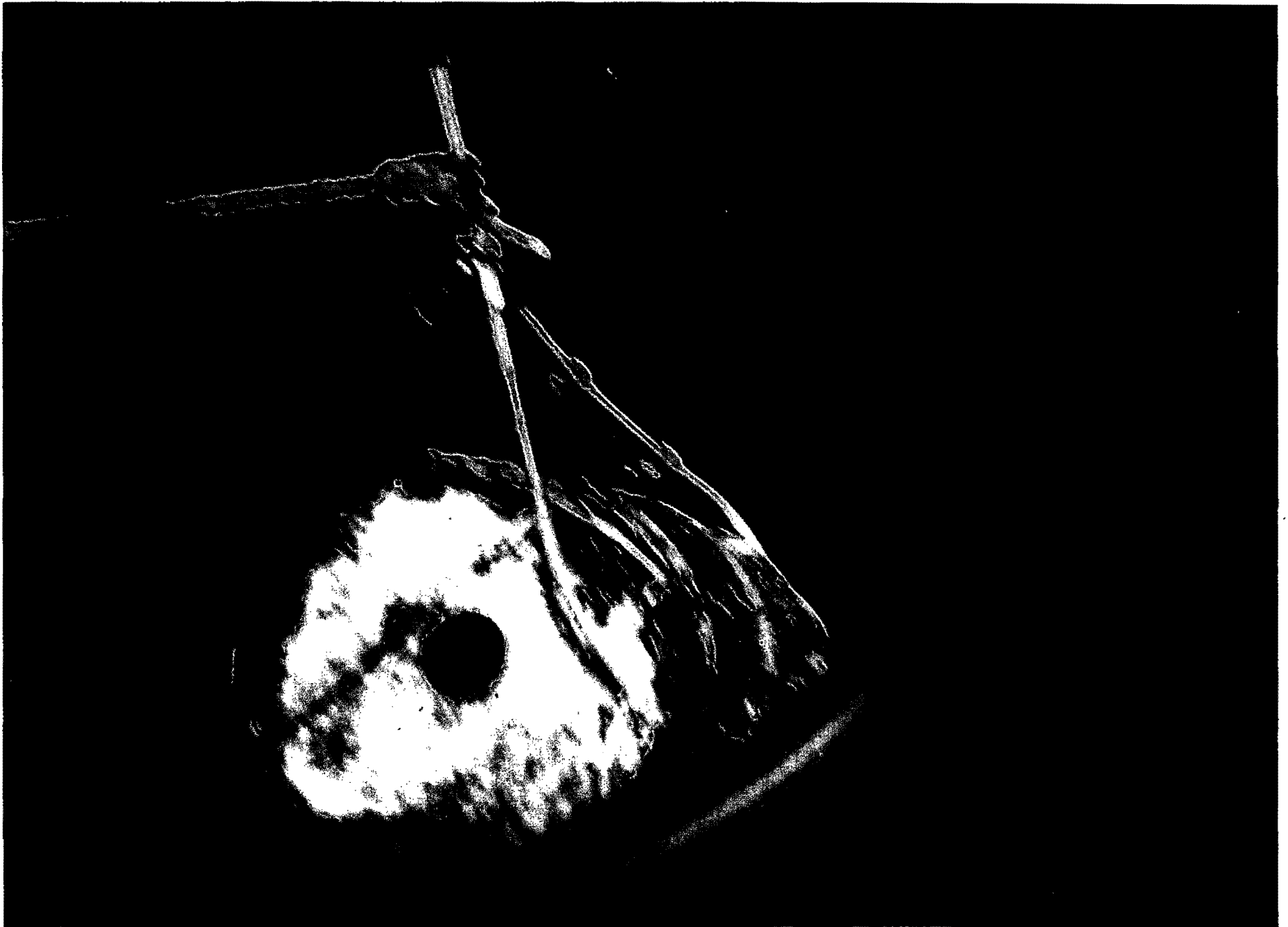
Figure 6   After clearing the surface, the waste package was subjected to a radiation survey prior to be taken aboard the R/V Advance II.

Figure 7   Following visual examination the package was transferred to a sealed storage container to inhibit further corrosion prior to laboratory analysis.

13

3. ANALYSIS OF THE CONCRETE WASTE FORM

3.1 Description of the Retrieved Waste Package

The waste package consisted of a 210-liter (55-gallon) container filled with Portland cement concrete. The diameter of the concrete waste form was 57.8 centimeters; its length was 85.1 centimeters. It weighed 306.8 kilograms. Imbedded into the center of the concrete waste form and running the entire length was a 7.6-centimeter (3 inch) diameter steel pipe. One end of the pipe was exposed to the concrete surface of the waste form. Common practice in preparing waste packages for ocean disposal was to cap the containers with "clean" concrete for radiation shielding and to minimize contamination during storage and transportation. The exposed pipe and the unfilled portion of the container (Figures 6 and 8a) indicate that the cap is missing. Judging by the weathering on the exposed concrete face and the debris found inside the pipe (such as pebbles and sediment indigenous to the environment at the package location) it is assumed that loss of the concrete cap may have occurred during descent or upon impact of the waste package with the ocean floor. Although there appears to be indications of erosion on the exposed concrete surface (Figure 8a), it is minimal considering the turbidity and bottom current velocities near the package. Figure 8b shows the condition of the bottom rim of the container and part of the sea side to the left of the yellow markings.

3.2 Concrete Coring

After removal of the mild steel container for corrosion studies, cores were taken of the concrete waste form to determine the types, quantities and distribution of contained radioactivity. Cores were taken from three locations along each of the 90° and 270° longitudinal axes extending to depths that approached the position of the embedded steel pipe. Orientation of the waste form and positions of the cores taken from it are shown in Figures 9a-9b.

15
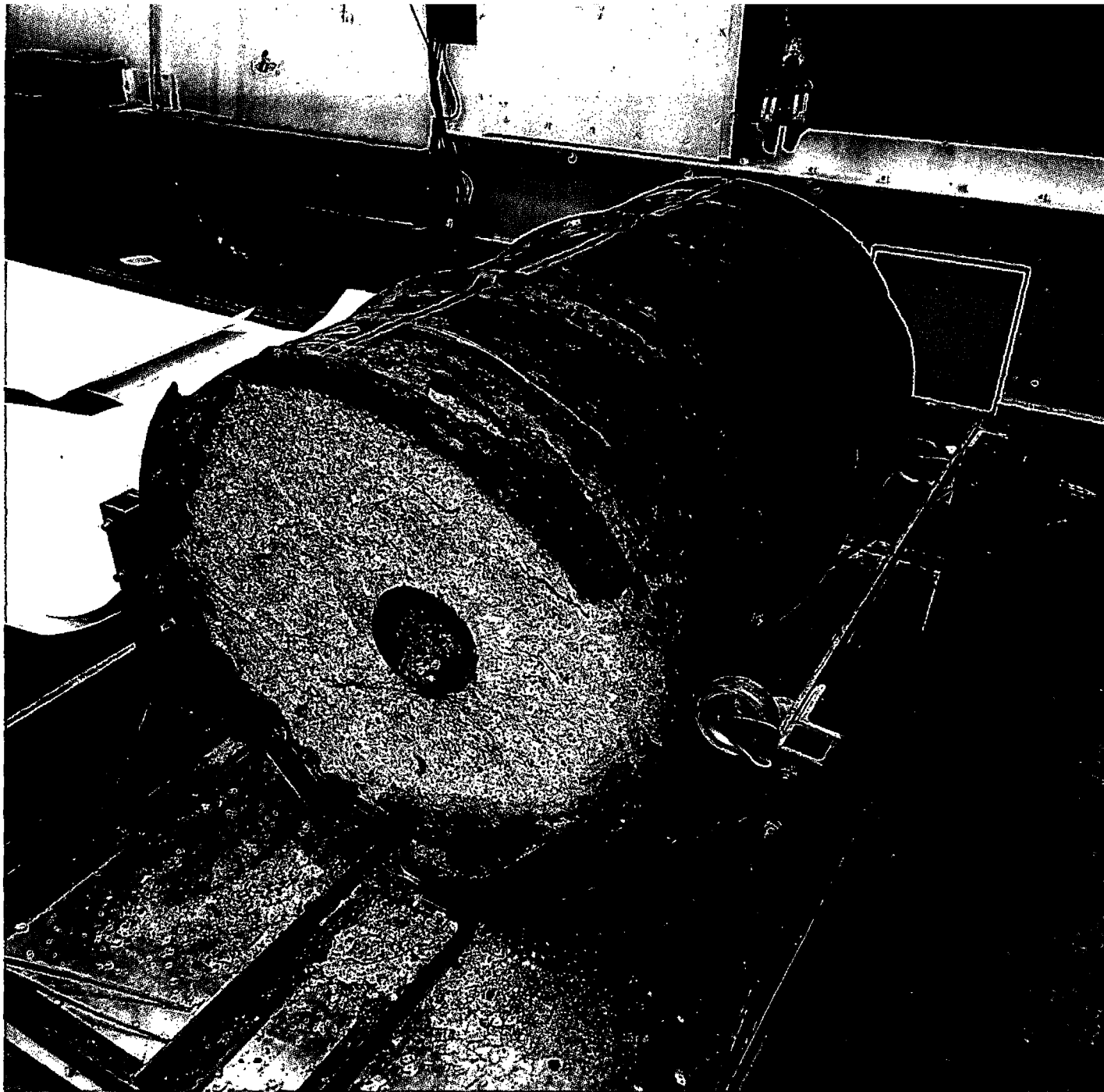
Figure 8a   Shows an exposed mild steel pipe which ran the entire length of the container and the weathered concrete surface.

Figure 8b   Overall view of the container showing the bottom side and the "markings" on the sea side.

17

Sediment Line

0°

270°

90°

180°
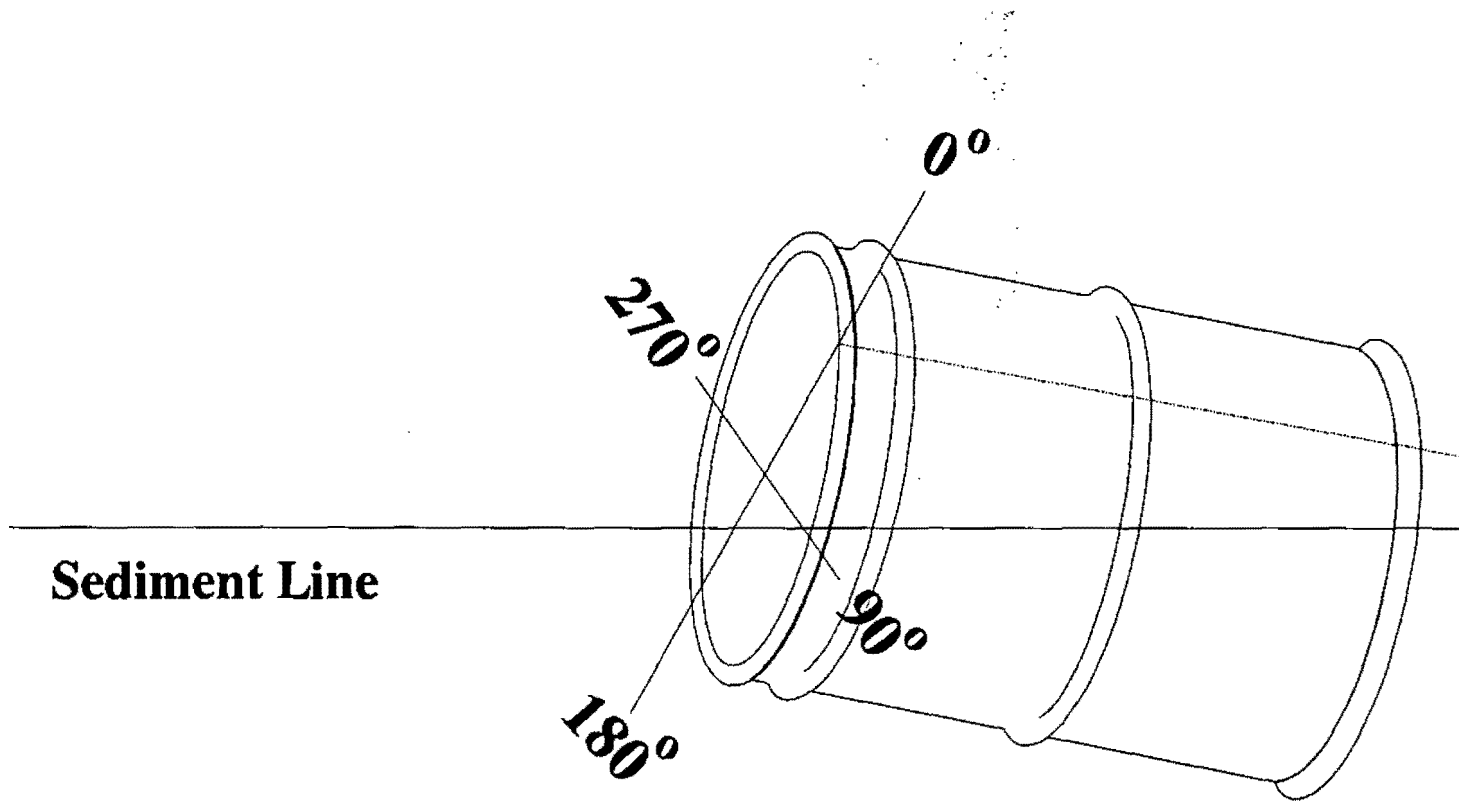
Figure 9a   Orientation of the waste package.

270°

| 270 | 271 | 273 |

| 91 | 92 | 93 |

90°

Core Locations
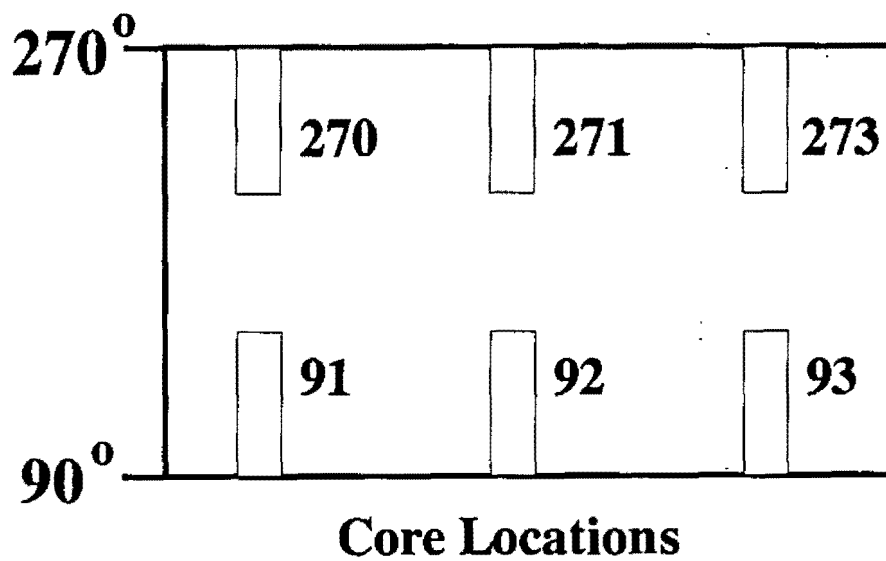
Figure 9b   Position of cores taken from the concrete waste form for analysis.

The concrete waste form was cored by a Target* concrete saw with a dual-speed motor (500/1000 rmp) on a swivel base. Impregnated diamond core bits (2-1/4 inch diameter) were used to produce two-inch diameter cores. Although water is normally used during concrete coring to both lubricate and to flush out debris, it was not used during this coring in order to minimize spraying and accumulation of contaminated liquid waste. Instead, a commercial teflon spray was periodically applied to lubricate the outside of the coring bit. This equipment and procedure was successfully used to obtain cement cores as previously reported [1,2]. However, due to the nature of the concrete composition (Table 2) and the lack of integrity, it was not possible to obtain satisfactory core samples for determining mechanical properties such as compressive strength. Based on its behavior, the compressive strength of the concrete waste form was estimated as <800 pounds per square-inch (5.515 MPa).

Weighed concrete samples removed from the waste form were digested in aqua regia, as described in Section 3.3. During this process, the aggregate was released from the cement matrix and the weight of the aggregate and (by difference) the cement were determined. These results are shown on Table 2, along with aggregate and cement percentages. The average contents of aggregate and cement were 61.3 and 38.7 percent, respectively. The distribution of cement content ranged from 22.4 to 66.2 percent, indicating that the waste form was not homogeneous when prepared for disposal due to improper mixing of cement, aggregate and waste.

3.3 Radiochemical Analysis

The concrete cores taken to determine radionuclide distribution in the waste form were dissolved in aqua regia prior to analysis. The aqua regia was made by combining 3 parts of 12$\underline{M}$ hydrochloric acid, 1 part of 16$\underline{M}$ nitric acid, and 1 part of distilled water by volume. Distilled water was added to inhibit the interaction of the

---

* Robert G. Evans Company, Kansas City, Missouri 64130.

TABLE 2
Cement and Aggregate Content of the Waste Form
Retrieved from the Atlantic 3800 Meter Site

Sample	Weight of core (g)	Weight of aggregate (g)	Weight of cement (g)	% Cement	% Aggregate
91-1	197.74	128.77	68.97	34.88	65.12
91-2	122.93	80.53	42.40	34.49	65.51
91-3	85.52	66.34	19.18	22.43	77.57
92-1	172.02	108.58	63.44	36.88	63.12
92-2	102.74	67.85	34.89	33.96	66.04
92-3	68.14	41.57	26.57	38.99	61.01
93-1	141.09	85.16	55.93	39.64	60.36
93-2	109.70	72.98	36.72	33.47	66.53
93-3	103.17	50.80	52.37	50.76	49.24
270-1	64.33	34.62	29.71	46.18	53.82
270-2	119.97	66.87	53.10	44.26	55.74
270-3	72.42	41.17	31.25	43.15	56.85
271-1	70.85	23.93	46.92	66.22	33.78
271-2	91.75	65.59	26.16	28.51	71.49
271-3	125.81	80.12	45.69	36.32	63.68
273-1	75.77	51.92	23.85	31.48	68.52
273-2	73.49	50.51	22.98	31.27	68.73
273-3	247.63	141.13	106.50	43.01	56.99

two acids during storage. Since the concrete waste form was composed of portland cement, sand, and stone aggregate, only the cement phase dissolved in the aqua regia. However, all the activity in the cores went into solution since it is associated predominantly with the cement phase. No activity was noted in any aggregate samples counted.

In the dissolution process, the concrete core to be dissolved was weighed and then placed in a glass beaker to which aqua regia and a Teflon stirring bar were added. The solution was stirred until the sample was dissolved and present in the solution as a suspended floc, with the exception of the aggregate, which settled to the bottom of the beaker. The solution containing the floc was then poured into a 500-ml volumetric flask, which in all cases exceeded the volume of the dissolved sample. The beaker and aggregate were washed with additional aqua regia to remove any residual solution and/or activity. This rinse was also added to the volumetric flask along with additional aqua regia to bring the liquid level up to the calibrated volume. The liquid in the volumetric flash was mixed thoroughly, and a 250-milliliter sample was taken for gamma-ray analysis.

The dissolved cement samples were analyzed using an Ortec" coaxial Ge (Li) detector. The detector was horizontally mounted with an integral FET preamplifier, the signal of which was fed into an Ortec 472A spectroscopy amplifier. The detector has an efficiency of 20 percent with a resolution of 2 keV at 1.33 MeV. The energy spectrum was analyzed during a Tracor Northern'" TN 1700 multi-channel analyzer in the pulse height analysis mode. A hardwired peak search routine (ALI) was used for peak identification and peak area determination.

"Ortec, Inc., 100 Midland Road, Oak Ridge, Tennessee 37830.

"'Tracor Northern, 3551 W. Beltline Highway, Middleton, Wisconsin 53562.

The gamma-ray analysis indicated the presence of a number of radionuclides. Table 3 shows results for gamma emitting radionuclides commonly associated with low-level radioactive waste. Very low activities of Cs-137 and Co-60 were observed in the waste form. Three core sections (sections 91-1, 93-1 and 93-3) contained detectable amounts of Cs-137. Three other sections (92-1,92-3 and 271-3) contained observable quantities of Co-60. The inhomogeneous distribution of these radionuclides make interpretation of release processes impossible.

Experimental studies investigating leaching of radionuclides from portland cement waste forms have shown that Cs-137 will leach via diffusion through the porous cement [5]. Based on curves from experimental studies of Cs-137 leaching from cement waste forms in seawater, it was determined that a diffusion coefficient of 1.07×10^{7} cm^2/sec is a reasonable estimate for Cs-137 leaching [6]. The ALT computer code [7] was used to calculate the fraction of Cs-137 released from the waste form over the 20 years (7300 days) that it rested on the ocean floor. The model results indicate that 65.3 percent of the cesium would leach out in that amount of time. The model curve is shown in Figure 10. Cobalt, however, behaves differently in the high-pH conditions of a cement-based material and can be expected to remain in an insoluble form and, therefore, resistant to leaching.

Gamma spectroscopy also showed the presence of Pb-212, Pb-214, Bi-214, Ac-228, K-40 and, intermittently, Th-234 and Ra-226/U-235. All of these radionuclides occur naturally, although they and/or their parent radionuclides may have been placed in the waste form. Table 4 shows the activities observed for Pb-212 and Bi-214. The activity of Pb-212 ranges from 0.014 to 0.222 pCi/g of cement. Lead-212 is one of the daughter radionuclides in the Th-232 decay chain. It was observed at 238.6 KeV (43.1 percent abundance). It has a short half-life (10.6 hours) and is maintained by the decay of the parent Th-232.

TABLE 3
Activities of Cs-137 and Co-60 In Cores
Taken From The Waste Form Recovered From the Atlantic 3800 m Site

SAMPLE	WEIGHT (g)	Cs-137 (pCi/g)	Co-60 (pCi/g)
91-1	68.87	0.15	BDL
91-2	42.40	BDL	BDL
91-3	19.18	BDL	BDL
92-1	63.44	BDL	0.18
92-2	34.89	BDL	0.37
92-3	26.57	BDL	BDL
93-1	55.93	0.88	BDL
93-2	36.72	BDL	BDL
93-3	52.37	2.04	BDL
270-1	29.71	BDL	BDL
270-2	53.10	BDL	BDL
270-3	31.25	BDL	BDL
271-1	46.92	BDL	BDL
271-2	26.16	BDL	BDL
271-3	45.69	BDL	4.88
273-1	23.85	BDL	BDL
273-2	22.98	BDL	BDL
273-3	106.5	BDL	BDL

The Detection Limit varies from about 0.10 to 0.20 pCi/g depending on the mass of concrete that was digested.

Cumulative Fraction Leached

Time (Days in Thousands)
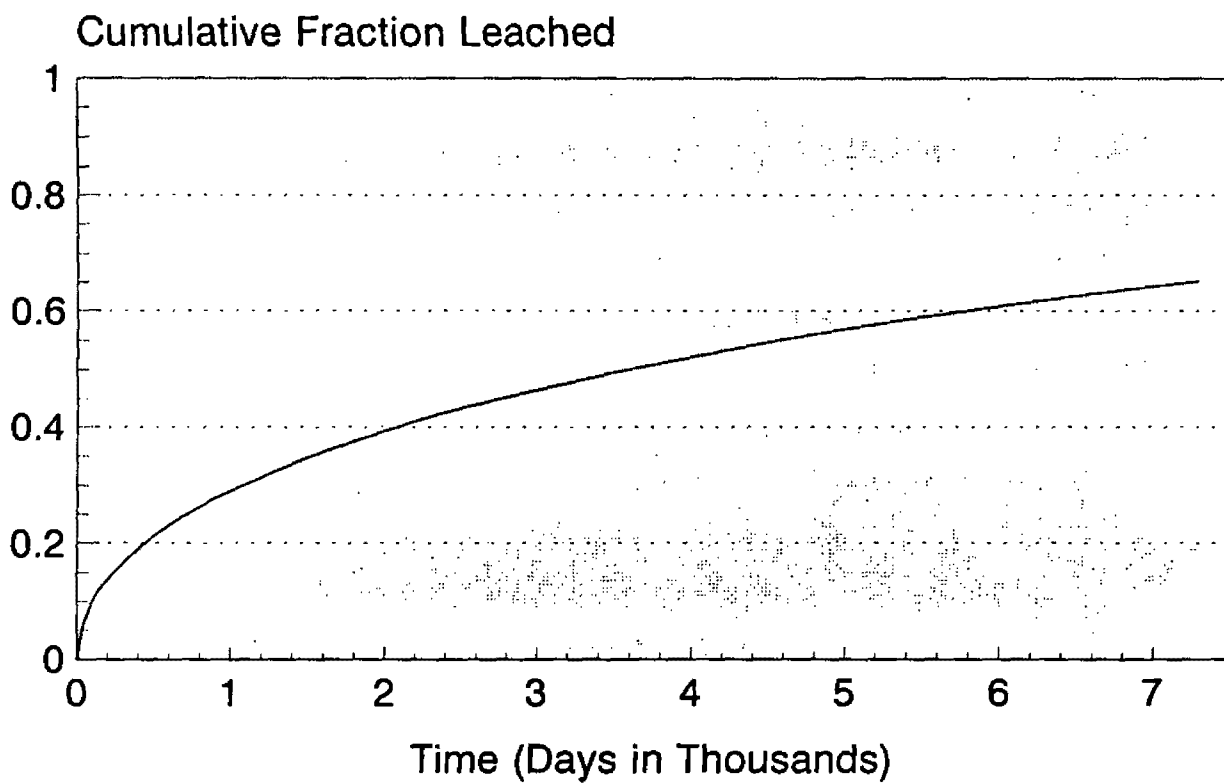
Leached in Sea Water
De=1.07 x 10^{-7} cm^2/sec

Figure 10   Modeled leaching of Cs-137 from a cement waste form; release after 20 years in water is 65.3%.

TABLE 4
Activities of Pb-212 and Bi-214 In Cores
Taken From the Waste Form Recovered From the Atlantic 3800 m Site

Sample	Weight (g)	Pb-212 (CPS)	Bi-214 (CPS)	Pb-212 (pCi/g)	Bi-214 (pCi/g)
91-1	68.87	0.0073	0.0018	0.088	0.056
91-2	42.4	0.0057	0.0019	0.112	0.096
91-3	19.18	0.0051	BDL	0.222	BDL
92-1	63.44	0.0075	0.0011	0.098	0.036
92-2	34.89	0.0043	0.0024	0.104	0.015
92-3	26.57	0.0023	0.0030	0.072	0.240
93-1	55.93	0.0024	0.0031	0.036	0.118
93-2	36.72	0.0062	0.0019	0.142	0.110
93-3	52.37	0.0027	0.0040	0.044	0.162
270-1	29.71	0.0029	BDL	0.082	BDL
270-2	53.1	0.0066	0.0027	0.104	0.108
270-3	31.25	0.0043	BDL	0.116	BDL
271-1	46.92	0.0039	BDL	0.070	BDL
271-2	26.16	0.0046	BDL	0.148	BDL
271-3	45.69	0.0052	0.0029	0.096	0.134
273-1	23.85	0.0033	BDL	0.116	BDL
273-2	22.98	0.0020	BDL	0.072	BDL
273-3	106.5	0.0018	0.0061	0.014	0.122

BDL, Below Detection Limits.

Bismuth-214 ranges in activity from 0.036 to 0.240 pCi/g. It is a daughter in the uranium-238 decay series, with a half-life of 19.7 minutes and is therefore maintained by the decay of U-238. It was observed at the 609.3 KeV line (46.1 percent abundance) and the 1120.3 KeV line (15 percent abundance). These radionuclides (Pb-212 and Bi-214) can be used in gamma spectroscopy as indicators of the presence of their parent radionuclides. The parents have only very low energy and/or low abundance gamma rays that are difficult to detect.

The presence of U-238 and Th-232 could be due to one of several possibilities:

1. These elements are naturally present in the raw materials from which the cement was produced;
2. U/Th or Ra waste was mixed into the waste form; or
3. The chemical nature of the cement concentrated some of these radionuclides as seawater moved into the waste form. This last hypothesis is the least likely.

To determine if the U-238 and Th-232 concentrations supporting the Bi-214 and Pb-212 are at environmental levels or higher (due to their presence in the waste), the Origen 2 computer code (version 2.1) was used. This code is typically used to calculate activities and masses of radionuclides generated in nuclear processes, such as those that take place in nuclear reactors. It can also be used to determine the quantities of daughter radionuclides resulting from the decay of natural radionuclides. During the modeling, an assumption of 1 gram of Th-232 or U-238 was made, and each was allowed to decay until it was at secular equilibrium with the daughters. The ratio of daughter to parent was then adjusted with the activity of the daughters observed in the waste form to give the activity and mass of the parents.

Lead-212 came into secular equilibrium with Th-232 rather rapidly, requiring between 50 and 100 years. Based on the measured quantity of Pb-212, it is estimated that the mass of Th-232 ranges from 1.3×10^{7} g/g of cement to 2×10^{6} g/g of cement.

The activity of Bi-214 comes into secular equilibrium with U-238 after approximately 1×10^{6} years. Assuming that there was no separation of uranium and bismuth, the activity of Bi-214 indicates that the mass of uranium ranges from 1.2×10^{7} g/g of cement to 8×10^{7} g/g of cement. It is reasonable to assume that the uranium is natural and has not been chemically separated, as one might suspect in a waste. This is because of the very slow in-growth of Bi-214. The activity of Bi-214 observed in the waste form would require a large mass of uranium to support it, if it had been separated recently. For example, if it had been effectively separated 20 years prior to analysis, the observed maximum Bi-214 activity would require 4.9×10^{4} g/g of cement. This is obviously impossible. The conclusion is that the uranium and thorium concentrations observed in the waste form are typical of those expected in naturally occurring materials.

4. CORROSION ANALYSIS OF THE METAL CONTAINER

As stated in previous reports [1,2], the corrosion analysis assesses the effect that the disposal site environment has upon the carbon steel sheathing material. Although one assumes total loss of this sheath, experience has shown that the sheath remains intact for very long periods of time and retards the leach rate by an observable amount. This aspect provides further motivation for studying the corrosion of the sheath material.

The method of corrosion analysis of this waste package follows the procedures described in previous reports [1,2] and includes the following tasks:

- Visual Inspection
- Dimensional Analysis
- Micro-Analysis
- Chemical and Metallurgical Analysis

4.1 Visual Inspection

As a result of visual inspection, one could see evidence of greater attack on the mud- buried portion than the side exposed only to the water. Figure 11 shows a schematic of the container and indicates how the container rested in the bottom sediment. As illustrated in Figure 11, the sediment intersects the package at the line ABCD corresponding to respective coordinates: $(x,r,\theta)=(0,28.6$ cm,25$^\circ)$, $(82.6$ cm,28.6 cm,56$^\circ)$, $(82.6$ cm,28.6 cm, 190$^\circ)$, $(0,28.6$ cm,200.4$^\circ)$. The arc's B, 90°, A and C, 90°, and D represent the portion of the container exposed to the sediment. Figure 8b shows a clear transition between the attached sediment side at angles less than 190° and the protected region corresponding to angles greater than 190°. Figure 12 shows a closer view of the difference between the sediment side, which exhibits severe general corrosive attack, and the more protected sea side. The corrosive
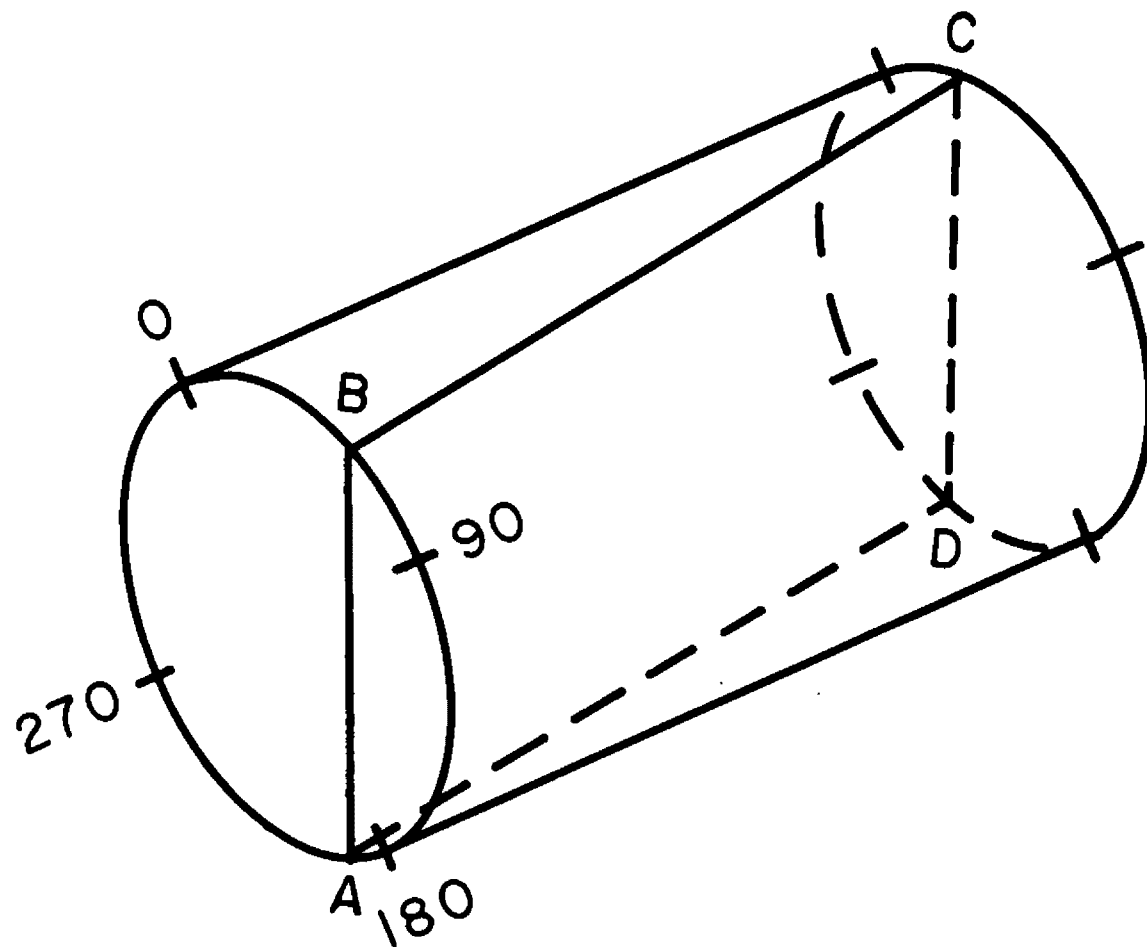
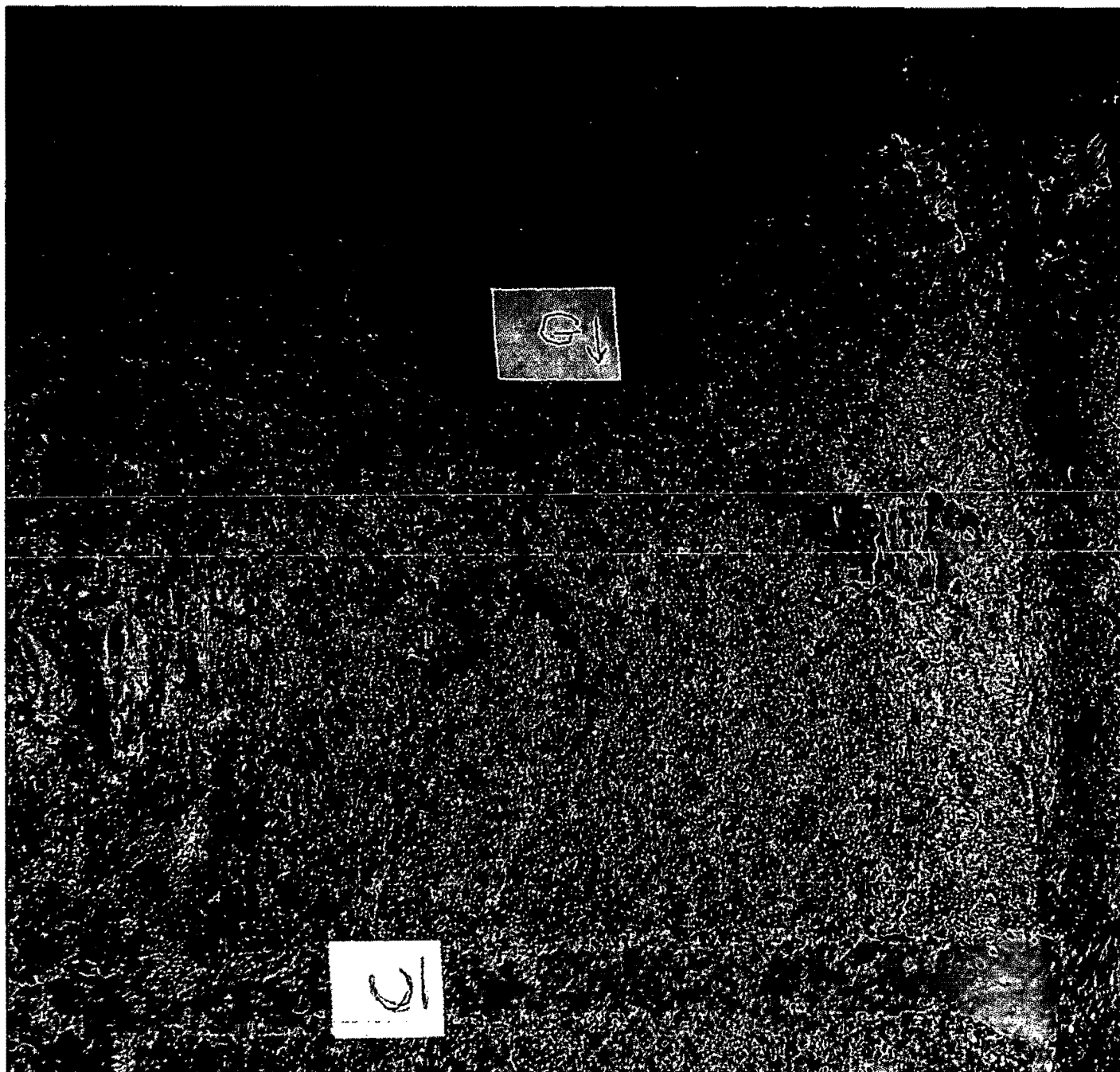Figure 11   Schematic of mud-line on the container.

Figure 12 Close view of severe general attack on sediment side compared to the more protected sea side.

31

attack goes from a pitting mode slightly above the sediment line (~190°) to a more generalized attack below the line. The attack below the sediment line shown in Figure 13 takes the form of a severe general pitting, while that on the sea side, Figure 14, appears more or less protected, possibly due to a coating. Figure 14 shows about a 0.1-millimeter diameter blistering of an apparent "coating." An instance of initiation of corrosion appears where a scratch is present.

Although the sea side exhibited less general attack, there were locations of specific high corrosion rates. For example, Figure 15 shows the chime near the top end of the container between 270° and 0°. This falls on the sea side. The chime exhibits an accelerated attack with a buildup of orange product, appearing to the left of a number "953," originally painted as an identification mark on the container. Figure 16 gives a closer view of this chime attack. The pH of the underlying material indicated that small regions less than 0.5 centimeters in diameter indicated slight acidity as a result of active pits.

Figure 15 also shows the perforation that occurred at the end of the container, which exposed the concrete. A closer view of this attack is seen in Figure 17. This rapid attack on the rim perforated the container at the sea and sediment-buried sides as well (Figure 18).

After extracting two strips, one from the sea side at 270° and one from the sediment side at 90°, two shells of the carbon steel sheath remained. Photographs of the inside of the shells appear in Figures 19a through 19c. Instances of perforation appear at the top of the container near the rim at the chimes and at the mud line. However, the perforation is less than 1 percent of the total sheath area, a somewhat better protection than was observed for the containers retrieved from the Atlantic 2800-meter site and the 900-meter Farallon Islands site [1,2] with respect to high localized attack.
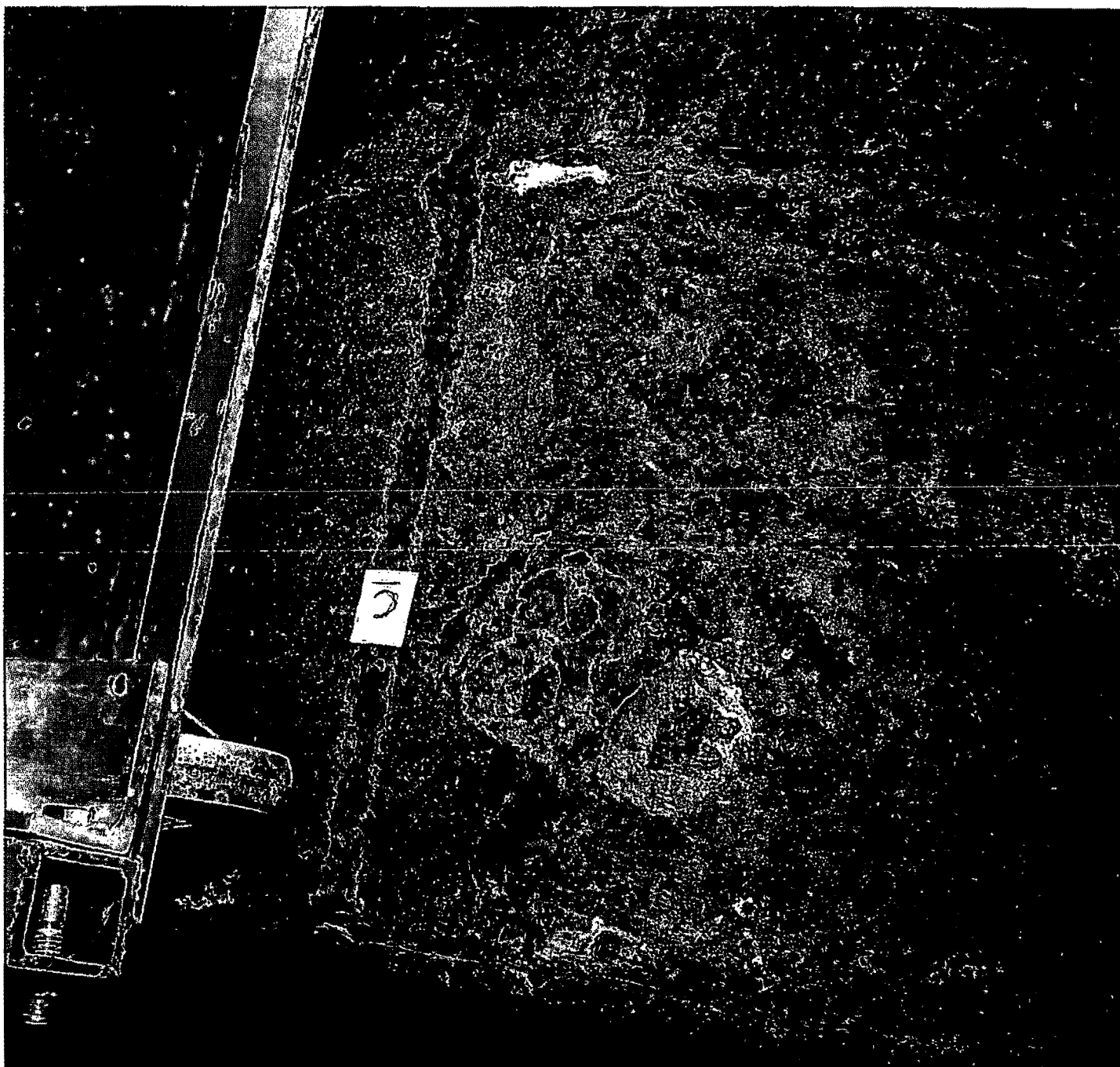
Figure 13   Severe general pitting below the sediment line.

Figure 14   Blistering of an apparent "coating" on the sea side of the container.
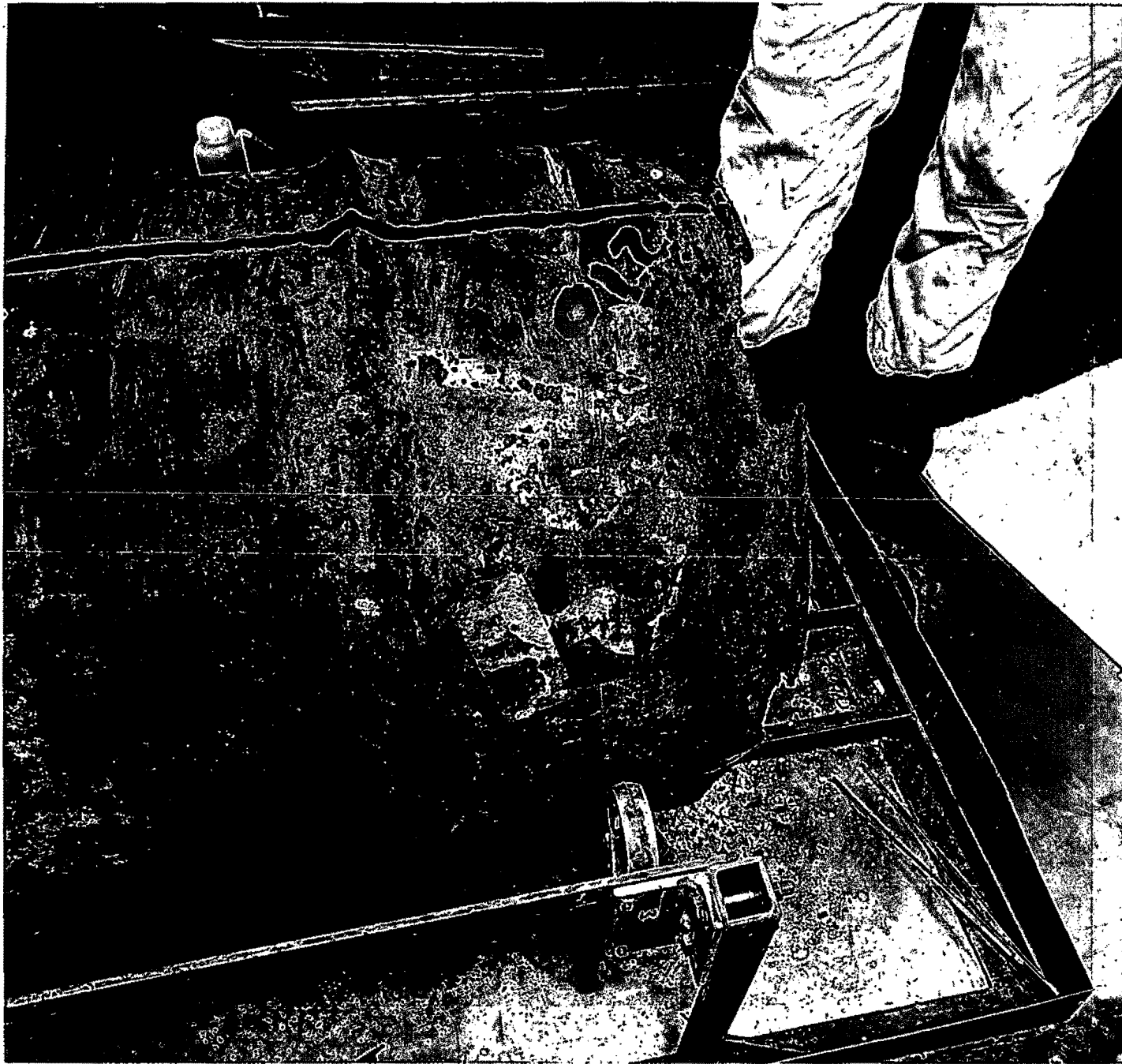
Figure 15 Accelerated attack near chime on sea side of container.

Figure 16   Close view of chime attack with buildup of orange product.

37

Figure 17   Close view of rim perforations.
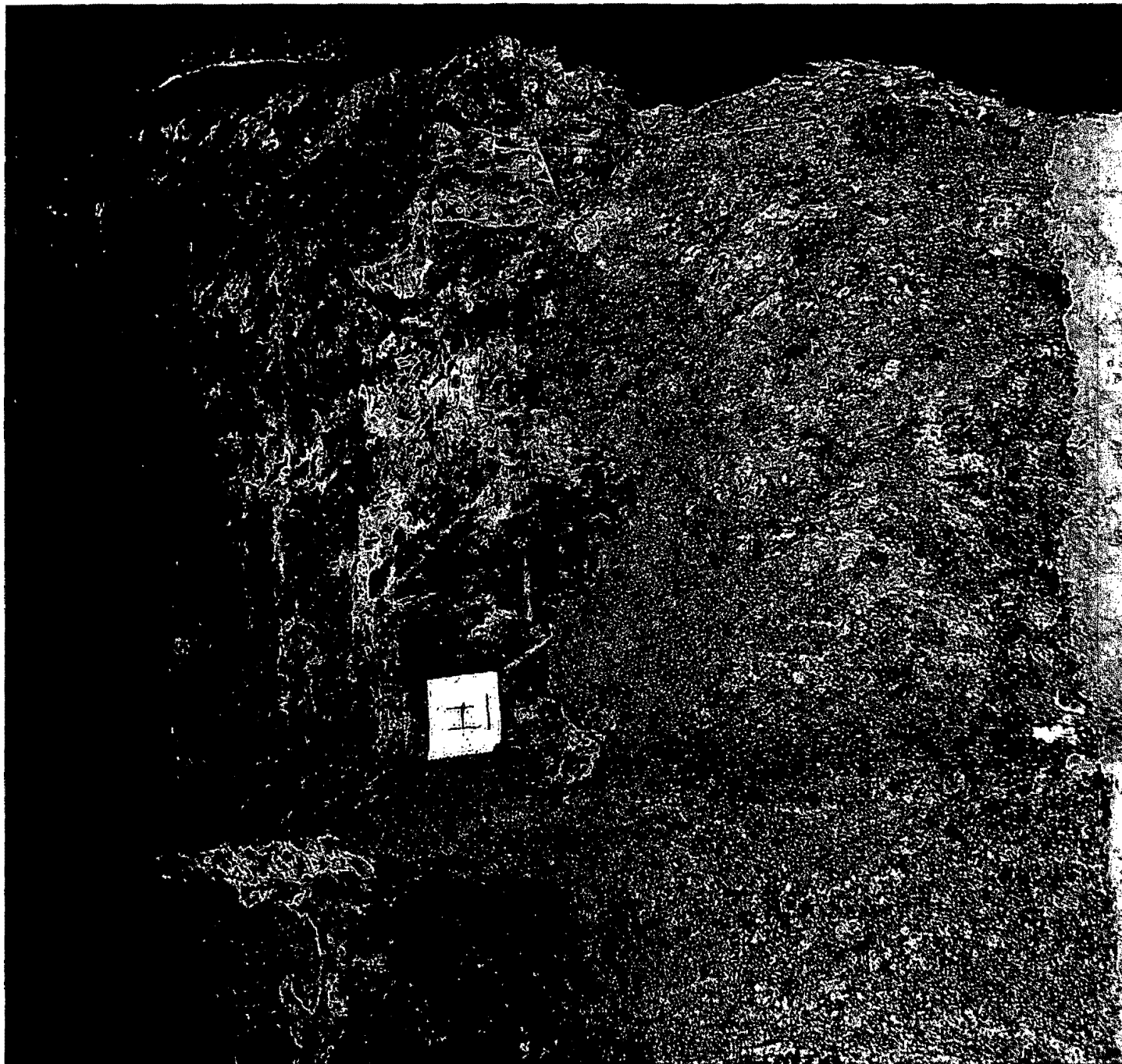
Figure 18   Upper rim perforations at the sea and sediment buried sides of the container.

Figure 19a   Photograph of inner side of sheath after removal from concrete. Perforations appear near rim of the chimes and at the mudline.

Figure 19b   Inner side of sheath showing perforations at the top of the container, at the chimes and at the mudline.
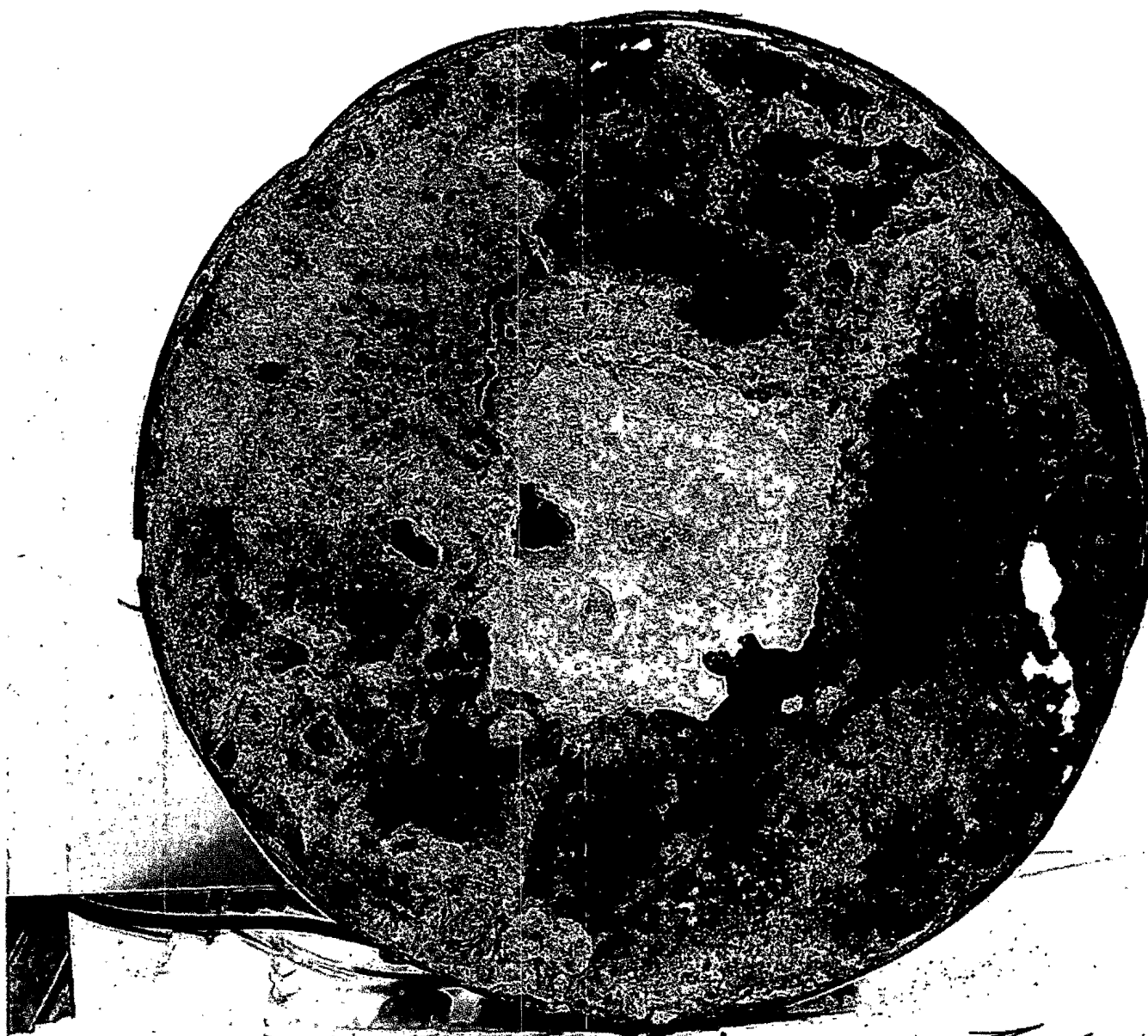
Figure 19c   Inside bottom of container showing perforations below the sediment line.

4.2 Dimensional Analysis

Strips cut from the respective sea and sediment sides of the carbon steel sheath provided specimens for dimensional analysis and metallographic examination. Specimens were extracted at 7.6-cm (3-inch) intervals along each strip, mounted in epoxy and ground past the saw cut damage with 320 sandpaper. The thickness from the photographed cross-section was measured at each 0.01-inch (0.025-cm) interval and averaged to obtain a dimension specific to each point taken at 7.6-cm intervals along the x direction. The standard deviation of the determination depends upon the localized nature of the corrosion. Large deviation indicates pitting.

Figure 19d shows the results plotted as metal thickness vs., x, the dimension down the container axis. In quantitative agreement with the qualitative visual observation, the sediment side shows a greater amount of metal loss than the sea side. The sediment side has an average metal thickness of 0.095 ± 0.015 cm and the sea side shows an average thickness of 0.116 ± 0.0095 cm. The majority of the metal loss on the sea side appears at either end of the package. The bottom at x=24 inches (60.6 cm) shows pitting. The middle of the sea side is protected, as was the case for previously-retrieved waste packages [1,2].

The initial dimension is unknown since the rim fold was compressed so that its dimensions fell under the maximum dimension of the thickest exposed portion. Hence, the initial dimension of 0.125 cm, the maximum observed thickness in the protection region, served as an initial dimension d_o, used to obtain the calculated corrosion rate, r:
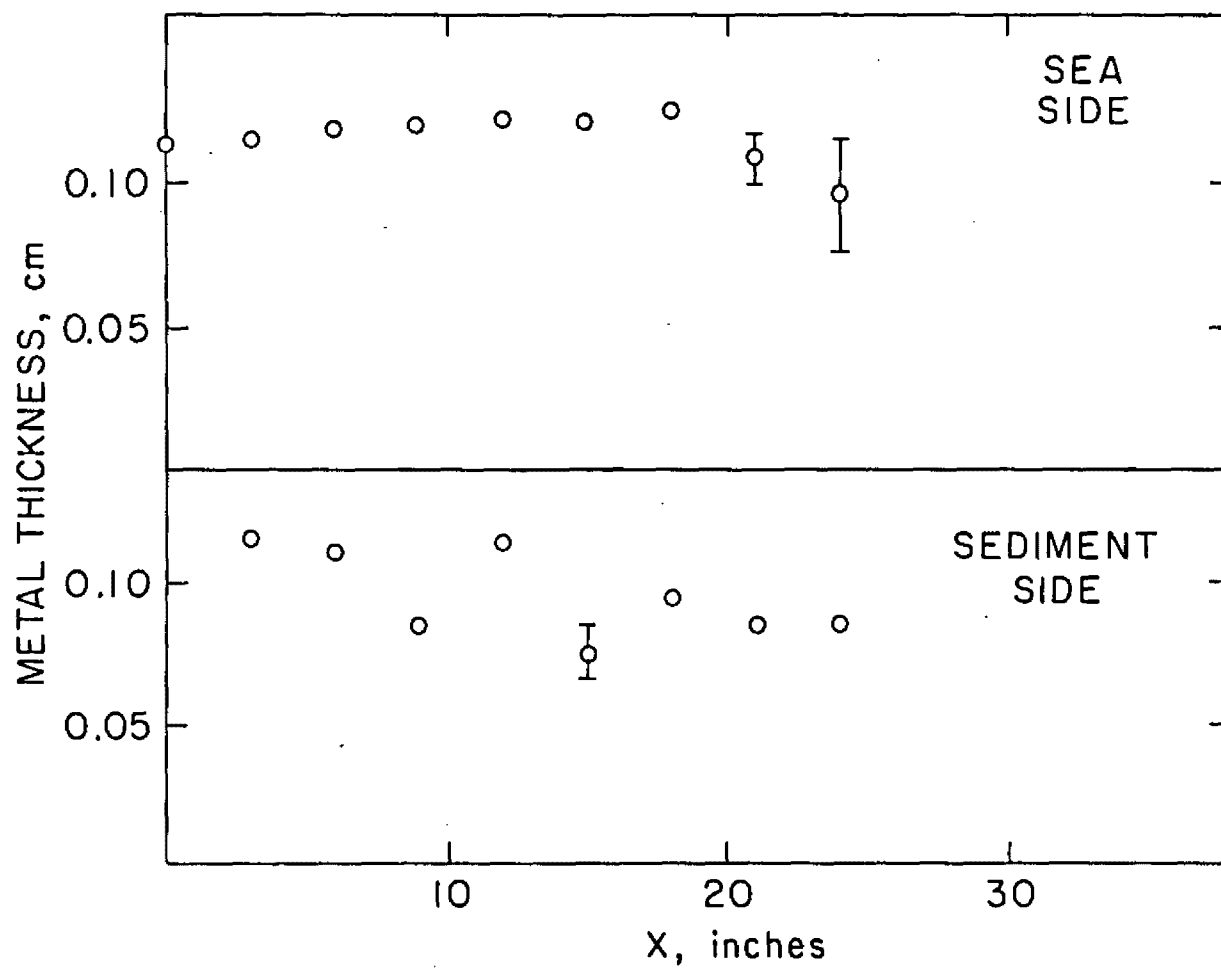
$$r = \frac{d_0 - d}{T}$$

Figure 19d   Plot of thickness of sheathing material vs. longitude.

where T is the time in the environment, taken as 20 years for this specimen. This gives a calculated corrosion rate of 0.015 ± 0.002 mm/year or 0.0006 ± 0.0001 in/year. The sea side exhibits an average corrosion rate too small to be determined by this macroscopic technique. One must keep in mind that these corrosion rates are based on the assumption of a constant rate over the period of time involved and should only be used as a means of comparing the different samples. Table 5 shows a comparison of the corrosion rates calculated for this container with the previous two retrieved from other Atlantic and Pacific radioactive waste disposal sites.

The calculated corrosion rate for the sediment side of this container is less than that observed for the container extracted from the Atlantic 2800-meter site and lies close to the zero-oxygen limit described by the empirical formula determined for specimens having well defined initial conditions [8]. To summarize the results of the dimensional analysis, the following statements can be made:

1.   The sediment side showed greater general corrosion than the sea side, with a rate of 0.015 mm/yr vs. <.005 mm/yr for the sea side. This corresponds to a time of 42 years to cause 50 percent loss at the sediment side.

2.   Nevertheless, the corrosion rate of the sediment side was close to that of empirically determined zero-oxygen limit.

3.   The general corrosion rate of the sediment side fell under that for the package retrieved from the 2800-m Atlantic site.

As mentioned before, both the sea side and the sediment side experienced perforation. These corrosion rates apply only to general attack, not to the high rate localized attack that produces perforation.

| TABLE 5			
Corrosion Rate Data for Waste Packages Retrieved from Deep Sea Disposal Sites			
Waste Package	Corrosion Rates inches yr^{-1}	Corrosion Rates mm yr^{-1}	Reference
Atlantic 2800-meter Site			

Gen. Attack
    Sea Side
    Sediment Side
Local Attack
	
	0.0013 ± .0002
	0.0019 ± .0002
	> 0.0026
		
		0.033
		0.048
		> 0.066
			(1)

Pacific 900-meter Site			

Gen. Attack
    Sea Side
    Sediment Side*
Local Attack
	
	0.00075 ± .00015
	0
	> 0.0021
		
		0.019
		0
		> 0.054
			(2)

Atlantic 3800-meter Site			

Gen. Attack
    Sea Side
    Sediment Side
	
	< 0.0002
	0.0006 ± 0.0001
		
		< 0.0045
		0.015
			This report

*Microscopic examination suggests a shallow pitting and scale formation resulting in a calculated 0.0025 mm/yr average.			

4.3 Micro-Analysis

Microscopic examination revealed specific attack or mechanisms of protection.

4.3.1 Protected Regions

The concrete/metal interface and the side not buried in the sediment experienced the greatest protection. Hence, these regions were closely examined to determine possible modes of protection. Figures 20a and 20b show the well-protected region of the container sheath at the concrete/metal interface from the portion of the drum not buried in the sediment. This particular sample has the following coordinates: (r=11.25 cm, x=21 cm, θ=270°). An apparent coating with a thickness of 5 to 7 microns (μ) covers the metal. Energy dispersive x-ray analysis (EDAX) revealed that the layer or "coating" directly covering the metal contained no heavy metals other than iron. However, deposits on this inner coating (Figure 20c) contained calcium, aluminum and chlorine deposits attributed to sea and concrete.

At the concrete/metal interface, the 5 to 7-μ film or "coating" remains continuous and adheres to the metal. However, on the environment side of this particular sample the 5 to 7-μ film or "coating" also remains continuous even over regions where a thick scale growth has produced a pit, Figure 21a. The scale growth on the pit exhibits cracks and voids, but the 5 to 7-μ initial film or coating remains, with the exception that a break appears above the center of the pit. In addition, a deposit lies over this 5 to 7-μ film or "coating" and contains compounds of aluminum and calcium, as shown in Figure 21b.

In a case where the thick, predominately calcium deposit remains, little corrosive attack has occurred. Also observed for this case, magnesium has concentrated in a layer closest to the 5 to 7-μ film under the outer calcium-rich deposit (Figures 22a and 22b). As shown by a considerable body of experimental data,

46
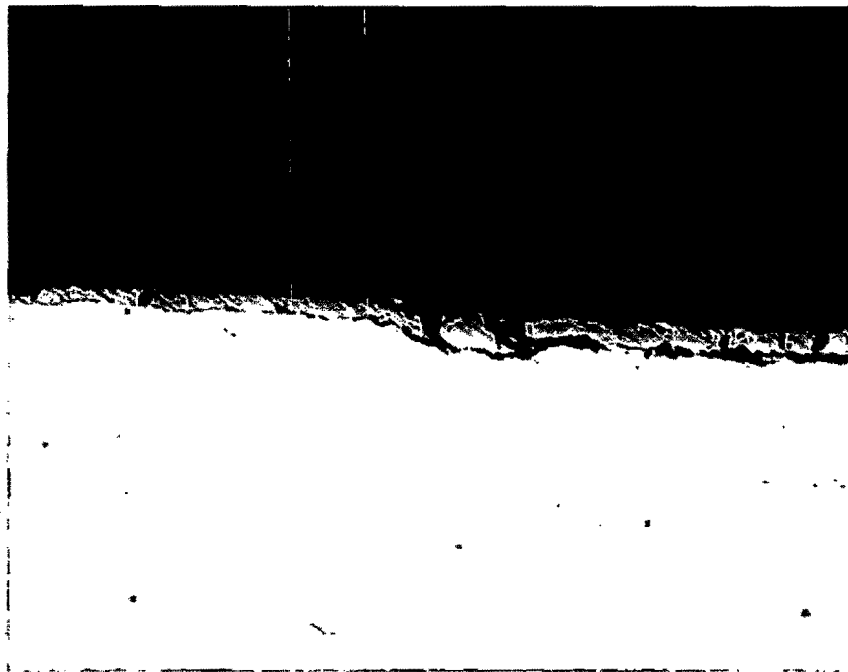
$0.002\ cm.$

Figure 20a   Optical photomicrograph of the metal/concrete interface from the well-protected portion of the container.
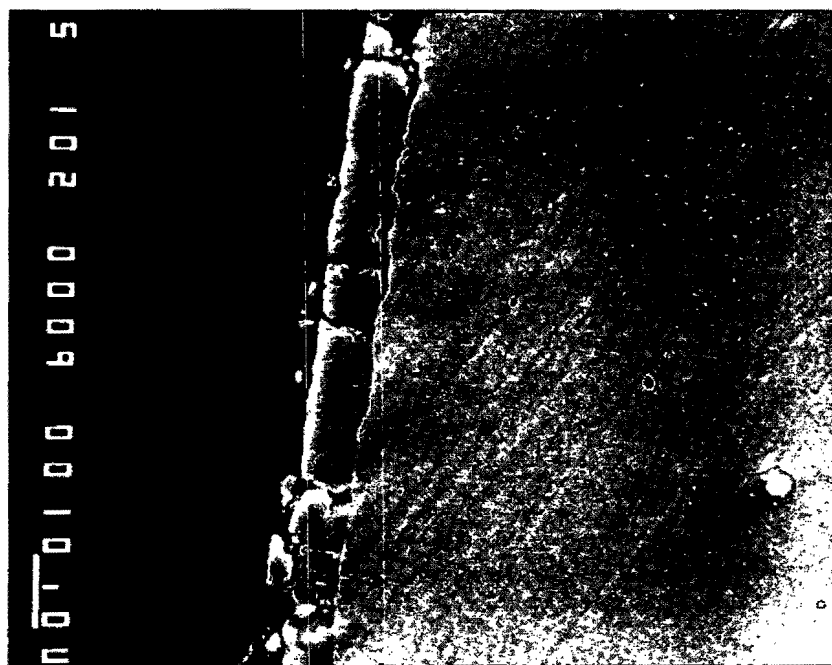

Figure 20b   SEM corresponding to the same area as 19a.

47

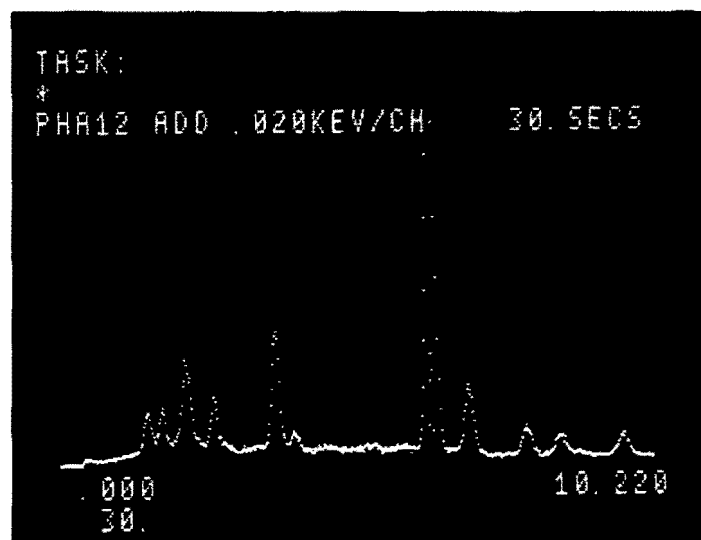Figure 20c   Energy Dispersive Spectroscopy (EDS) of deposits (Ca, Al, Cl, etc.) on the inner coating of the container sheath.
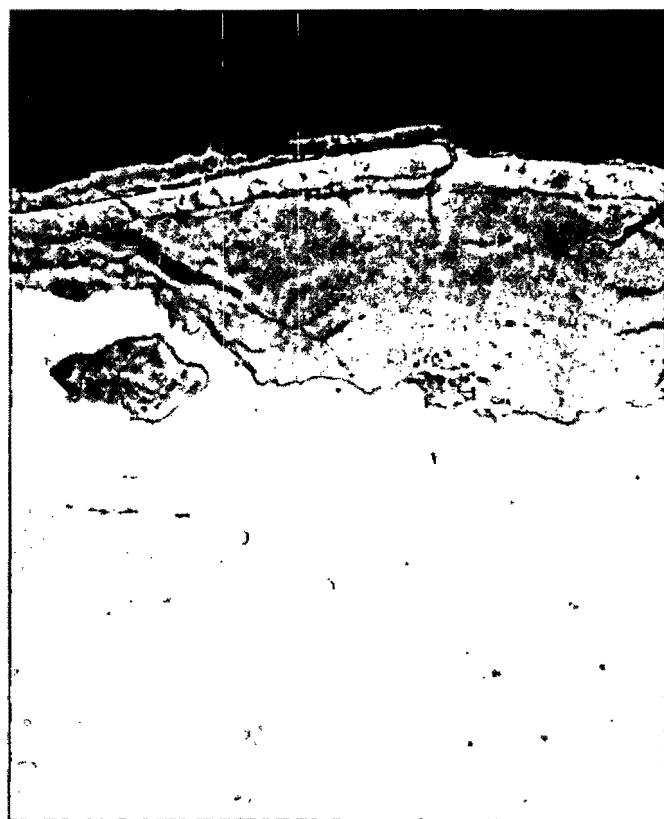
Figure 21a   SEM photograph of a pit initiated on the sea side of the container at R=11.25, x=21 cm, Θ=270°.

TASK:
*
PHA12 ADD .020KEV/CH   30. SECS

.000   10. 220
30.

Figure 21b   EDS of scale above 5-7μ film or "coating" showing Al and Ca compounds.

Figure 22a   SEM showing the distribution of elements in the scale formed on the sea exposed side of the well-protected region of the container.

Figure 22b   X-ray DOT mapping of magnesium layer.

alkaline earth precipitates can protect metal in the marine environment [9] because of diminished oxygen depolarization of the cathodic sites [10]. Conceivably, the oce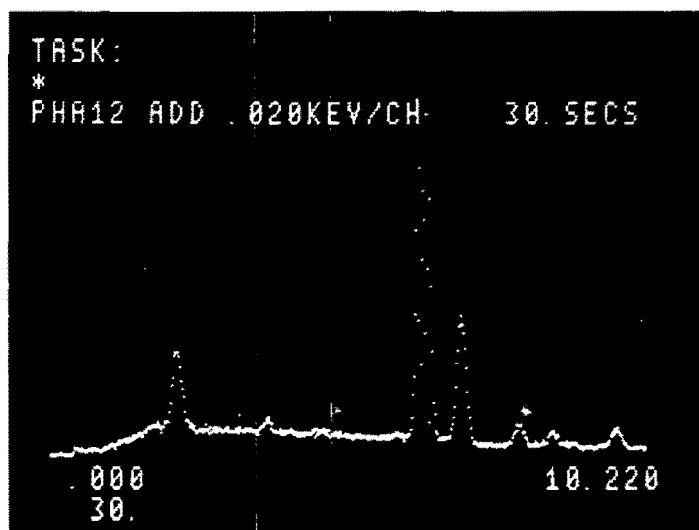an side of the container could be predominantly a cathode where the following reaction dominates, $2e^- + O_2 + 2H_2O \rightarrow 4OH^-$, and the anodic dissolution, $H_2O + Fe \rightarrow FeOH^+ +H^+ +2e^-$, would dominate the sediment side. Initially, this differential aeration between the sea and sediment sides will encourage these reactions. Precipitation of alkaline earth scale would slow the entire process, probably due to diminished mass transfer of the O_2 depolarization [11]. Although the ocean side shows better protection against general corrosion than the sediment side, high localized attack penetrated several places on this side. Specific penetration occurred at the rim of the end with exposed concrete and at several points on or near the chimes. Severe, but localized, pitting also occurred on the sea-facing side. Figure 23a shows an oxide-filled pit found on the side of the sheath facing the sea. The oxide is 0.02 cm thick at the maximum and appears to have grown in layers. It exhibits cracks, extending to the base of the pit. The base of the oxide contains "ghosts" of the metal, seen as light spots in the micrograph (Figure 23b). Scrutiny of the initial-etched sample by a scanning electron micrograph, Figure 23c, showed inclusions having the same morphology as the embedded "ghosts." EDS analysis, Figure 23d, indicates that these "ghosts" originate from the metal as grain boundary precipitated carbides.

4.3.2 Rapidly Corroded Region on the Sediment Side

While the ocean-exposed surface of the container provides regions of high protection, its sediment side showed the greatest metal loss resulting from general attack. This attack takes the form of a general pitting. The base of a typical pitted region in a sample taken from (x=38.1 cm, $\theta=90°$) shows the morphology of the attack (Figure 24). In contrast to the side above the sediment, this surface has porous, loosely adherent scale. The scale also contains some of the carbide "ghosts."

The concrete/metal interface of this specimen exhibited virtually no attack and contained the 5 to 7-μ film of "coating" (Figure 25). Thus, the concrete/metal interface
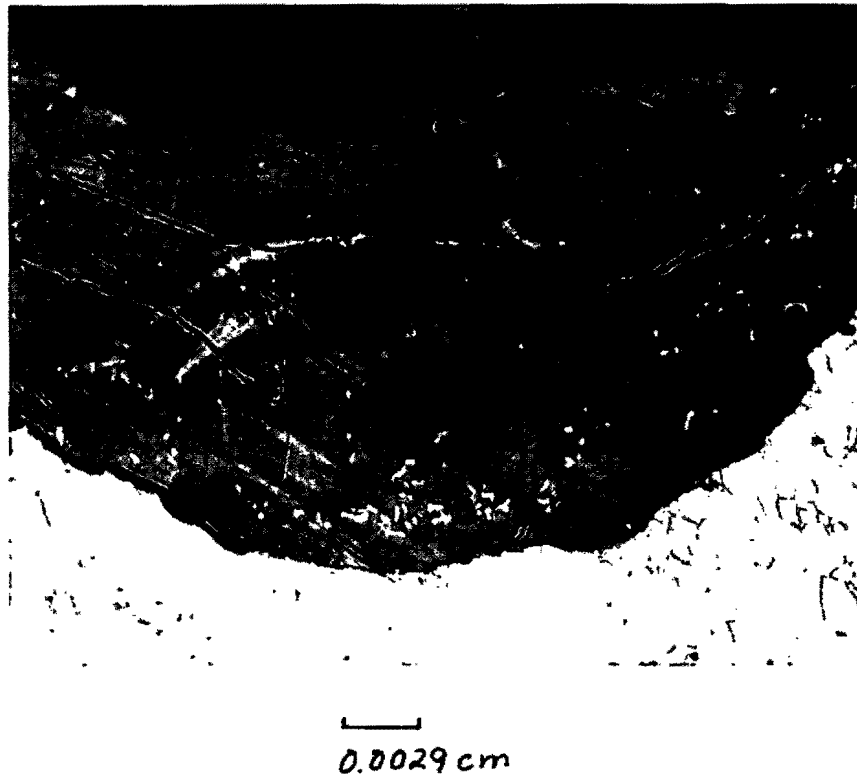
$\longmapsto$
$0.0029\,cm$

Figure 23a   Optical photomicrograph of an oxide-filled pit on the sea side of the container.
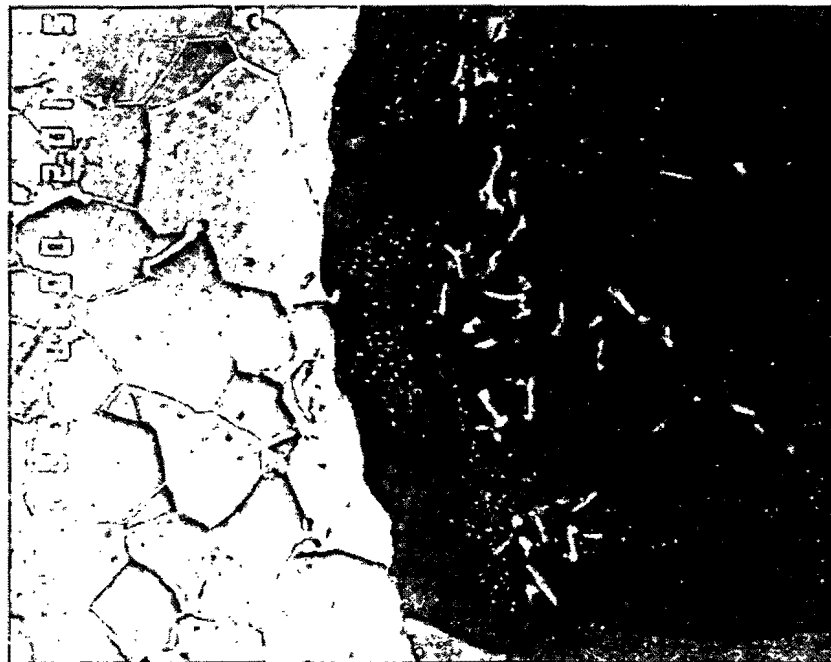
Figure 23b   SEM photograph of the same area showing metallic "Ghosts."

52

Figure 23c   SEM photograph of inclusions and precipitates in the metal.

Figure 23d   EDS analysis of inclusions and precipitates of the metal and the MnS inclusion.

0.0025 cm

Figure 24   Optical photograph of severe attack on a sample taken from the sediment side at
x=38.1 cm, Θ=90°

0.0025 cm

Figure 25   Optical photomicrograph of the concrete/metal interface at x=38.1 cm, Θ=90°.

over the entire package showed no attack except at the end of the container where the concrete was exposed.

4.4 Chemistry and Metallurgy

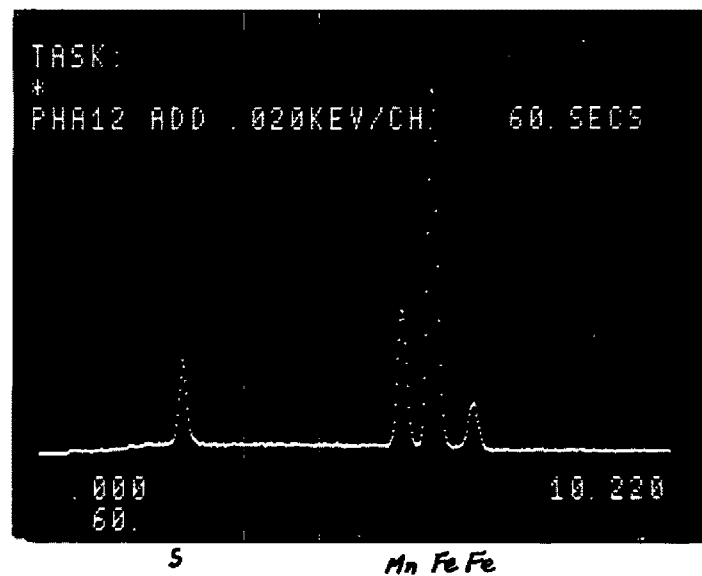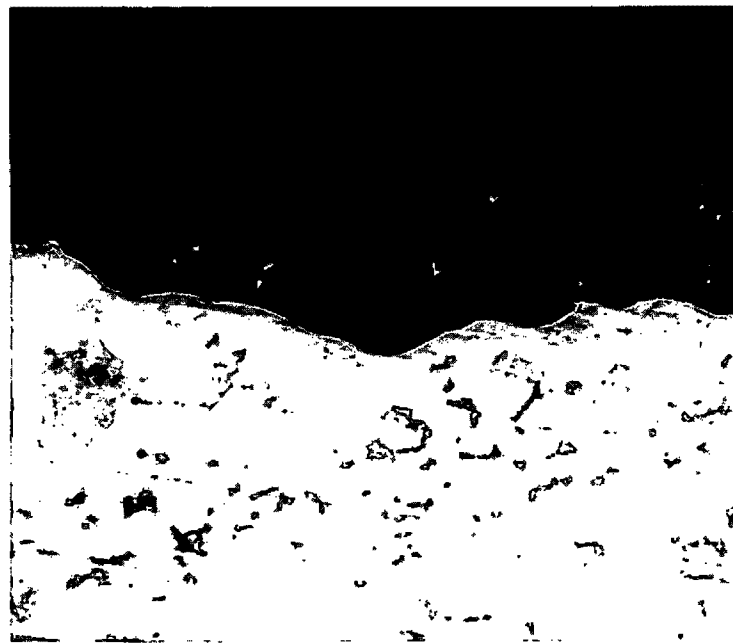Immediately after removal of the waste package from the sealed storage container, scrapings and samples were taken from regions indicating high corrosion rates (Table 6) to determine product composition. Table 7 shows the samples taken for x-ray diffraction (XRD) analysis. The samples consisted primarily of γ-Fe_2O_3 and γ-$Fe_2O_3H_2O$ which can form from a rapid oxidation of ferrous ions in neutral solution [12]. α-Ferric oxides also contributed to the composition of these scrapings.

The analyses of trace elements present in the carbon steel sheath (Table 8) did not differ significantly from that of a previous container retrieved from the 2800-meter site in the Atlantic Ocean [1]. Differences in corrosion rates can therefore be attributed to the respective environments. The metallurgy of the drum did not differ significantly from that of the two previously-retrieved containers (Table 8).

4.5 Discussion

The calculated rates provided by the dimensional analysis allow some interesting comparisons among the three samples. As stated in previous reports, the calculated rate results from the assumption of a constant rate over the entire time of storage of the package. This represents a rather severe assumption, but must be used to compare the different samples quantitatively. Under this assumption, the metal loss as a function of time would appear as the schematic, Figure 26a, the slope being determined by a chemical variable, O_2 concentration for instance. With similar composite systems [13], initiation and inhibition play important roles in determining the metal loss (Figure 26b). In general, there is an initiation time, a propagation period, and a possible inhibition at longer times.

	Position			
TABLE 6				
Position and Description of Container Scrapings and Samples				
Scraping No.	R, (cm.)	X, (cm.)	0 (degrees)	Comments
III-1	28.7	34.2	305	Corrosion product near chime
III-2	28.7	11.43	255	Adherent materials near rim
III-4	17.2	83	45	Corrosion product from container end
III-5	28.7	66	30	Deposit over perforation
III-6	28.7	15	170	Pits-orange molecule

TABLE 7	
X-ray Diffraction Identification of Surface Scrapings	
III-1	γ-Fe$_2$O$_3$ some α-FeO(OH)
III-2	γ-Fe$_2$O$_3$ and some other oxides
III-4	α-Fe$_2$O$_3$ H$_2$O α-Fe$_3$O$_4$ γ-Fe$_2$O$_3$ H$_2$O γ-Fe$_2$O$_3$
III-5	γ-Fe$_2$O$_3$, FeO(OH) α-FeOOH
III-6	γ-Fe$_2$O$_3$, γ-Fe$_2$O$_3$ H$_2$O

TABLE 8
Metallurgical Analysis of Waste Container

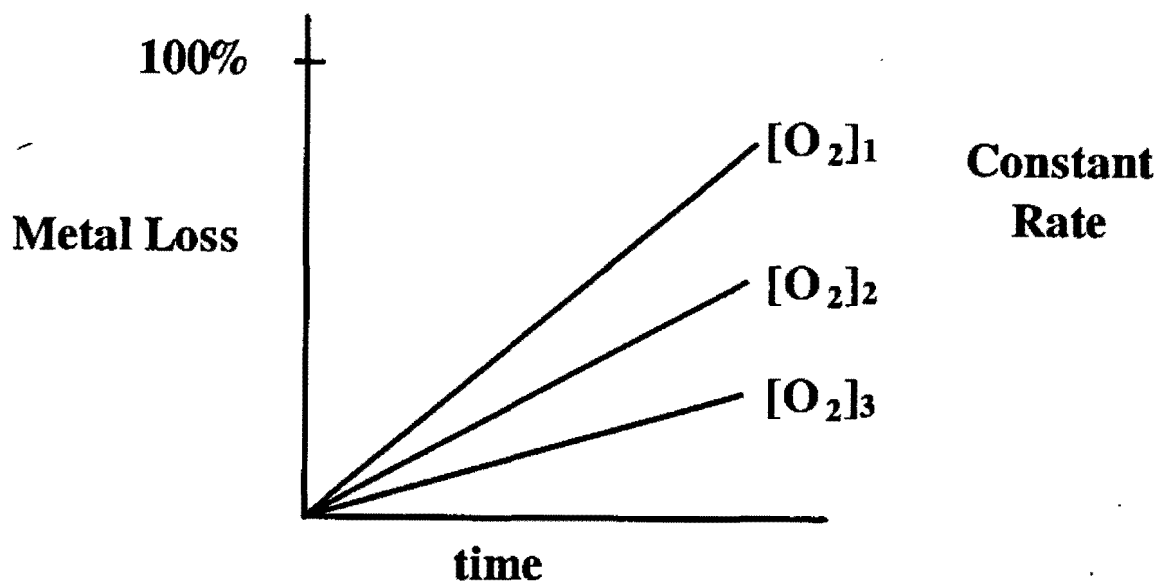| Element	Weight Percent
C	0.10
Mn	0.38
P	0.005
S	0.030
Si	< 0.02
Ni	< 0.02
Cr	< 0.02
Mo	< 0.02
Cu	0.1
Fe	Balance

Figure 26a   Schematic of metal loss vs. time assuming a constant corrosion rate.
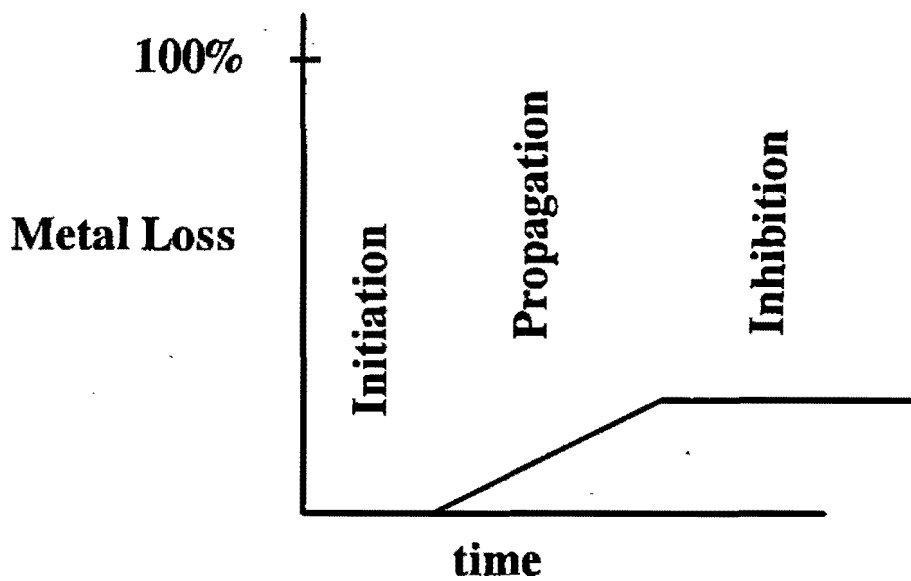

Figure 26b   Schematic of generalized corrosion kinetics.

Keeping in mind these above points, the "calculated rate" for this sample can be compared to data for other containers and data from the literature [1,2]. The summary of the general observations follow:

1. The sediment-facing surface showed greater metal loss than the sea side for this package. This is the reverse for the losses observed in the container taken from a 900-meter Pacific site.

2. The calculated rate for the sediment side is 0.015 ± 0.002 mm/yr (0.0006 ± 0.0001 in/yr) and corresponds to a 50 percent reduction in 42 years.

3. The rate observed for general attack of the sediment buried side is close to that for the Pacific container and to the zero-oxygen limit (see Table 5).

4. The rate observed for general attack of the sediment-buried side is significantly less than that for the greatest general attack experienced by the Atlantic container retrieved from 2800 meters.

Clearly, there are many factors involved that protect the container sheath from corrosion, since metal loss probably follows a law similar to the schematic in Figure 26b.

Coatings, cathodic depolarizers such as dissolved oxygen, inhibiting materials such as Ca^{2+} and Mg^{2+} precipitates, pH and ocean current all have effects. Part of the Atlantic 2800-meter container and the entire Pacific 900-meter container appear to have a coating that would contribute to the time to initiate corrosion.

The differences in oxygen concentrations appear to play an important role also. The Pacific 900-meter container, an apparently uncoated specimen, shows less loss than the uncoated portion of the Atlantic 2800-meter container. The sample comes

from a 900-meter Pacific site having a lower O_2 concentration than the 2800-meter Atlantic site from which a sample was obtained [2].

In addition, the mass flow of the cathodic depolarizer, O_2, to the metal surface and the precipitation of calcium and magnesium precipitates probably inhibit the cathodic process over the entire container. If the cathodic process is the rate-determining step, then this will control the corrosion rate. The effect of the Mg and Ca precipitates upon the cathodic process has been well established [9,10] and even provides the basis for a patent application [14]. Feigenbaum has used the high-frequency (>1KHZ) impedance across protective scale to assess the corrosivity of fresh waters [10]. Perhaps, this applies to this system and environment. If this were to be the case, a rapid in-situ probe could be easily developed.

4.6 Summary and Conclusion

The following summary and conclusions concerning the third container can be made at this time.

1. The loss of metal as a result of corrosion is greater on the sediment side than on the sea side. Assuming a constant rate (Figure 26a), the calculated rate is 0.015 ± 0.002 mm/yr. This corresponds to a 50 percent reduction of wall in 42 years. The general loss of the sea side is within the error of the measurement of average wall thickness.

2. An apparent coating and Ca^{2+} or Mg^{2+} precipitates appear to inhibit the respective initiation and propagation of corrosion for this material in this environment.

3. High local attack appears at chimes and at the rim of the concrete-exposed end, where loss of concrete to metal adhesion occurs.

61

5. REFERENCES

1. Colombo, Peter, R.M. Neilson, Jr. and M.W. Kendig, "Analysis of a Radioactive Waste Package from the Atlantic 2800 Meter Disposal Site," EPA 520/1-82-009, Office of Radiation Programs, U.S. Environmental Protection Agency, Washington, DC, May 1982.

2. Colombo, Peter and M.W. Kendig, "Analysis and Evaluation of a Radioactive Waste Package Retrieved from the Farallon Islands 900-Meter Disposal Site," EPA 520/1-90-014, Office of Radiation Programs, U.S. Environmental Protection Agency, Washington, DC, September 1990.

3. Hanselman, David S. and W.B.F. Ryan, "1978 Atlantic 3800-Meter Radioactive Disposal Site Survey -- Sedimentary, Micromorphologic and Geophysical Analyses," EPA 520/9-79-001, Office of Radiation Programs, U.S. Environmental Protection Agency, Washington, DC, June 1983.

4. Walden, Barrie B., "Recovery of Low-Level Radioactive Waste Packages from Deep-Ocean Disposal Sites," EPA 520/1-90-027, Office of Radiation Programs, U.S. Environmental Protection Agency, Washington, DC, September 1990.

5. Fuhrmann, Mark, R.F. Pietrzak, J. Heiser, E-M. Franz, and P. Colombo, "Accelerated Leach Test Development Program," BNL-52270, Brookhaven National Laboratory, Upton, NY, November 1990.

6. Fuhrmann, Mark and P. Colombo, "Radionuclide Releases from Cement Waste Forms in Seawater," Radioactive Waste Management and the Nuclear Fuel Cycle, Vol. II, No. 4, pp. 365-380, 1989.

7. Fuhrmann, Mark, J. Heiser, R. Pietrzak, E-M. Franz, and P. Colombo, "User's Guide for the Accelerated Leach Test Computer Program," BNL-52267, Brookhaven National Laboratory, Upton, NY, 1990.

8. Dyer, Robert S., "Environmental Surveys of Two Deep Sea Radioactive Waste Disposal Sites using Submersibles," Proc. Int. Symp., IAEA, Vienna (1976), 317-338.

9. LaQue, F.S., "Marine Corrosion," and references therein.

10. Feigenbaum, C., et. al., Corrosion Science, 34(4), 133 1978.

11. Reinhart, F.M., et. al., "The Relationship Between the Concentration of Oxygen and Seawater Corrosion of Metals," Proc. 3rd Cong. on Marine Corrosion, 1972, 562.

12. Misawa, T.K., et. al., Corrosion Science, 14, 131, 1974.

13. Tutti, K., "Cracks and Corrosion," Swedish Cement and Concrete Research Institute, Institute of Technology, Stockholm, ISSN 0346-6906, 1978.

14. Discussions with Drs. Hermann and Clayton, State University of Stony Brook; Dr. Hermann informed me that a Dr. Wolf Hibberts of University of Texas, Austin, has applied for such as patent.